A study on nitroimidazole-99mTc(CO)3 complexes as hypoxia marker: some observations towards possible improvement in vivo efficacy. Nucl Med Biol

ARTICLE *in* NUCLEAR MEDICINE AND BIOLOGY · AUGUST 2014

Impact Factor: 2.41 · DOI: 10.1016/j.nucmedbio.2014.04.103

5 AUTHORS, INCLUDING:

Madhava B Mallia
Bhabha Atomic Research Centre
33 PUBLICATIONS **286** CITATIONS
SEE PROFILE

Suresh Subramanian
Bhabha Atomic Research Centre
27 PUBLICATIONS **293** CITATIONS
SEE PROFILE

Haladhar Dev Sarma
Bhabha Atomic Research Centre
159 PUBLICATIONS **1,374** CITATIONS
SEE PROFILE

Sharmila Banerjee
Government of India
191 PUBLICATIONS **1,949** CITATIONS
SEE PROFILE

Nuclear Medicine and Biology 41 (2014) 600–610

Contents lists available at ScienceDirect

Nuclear Medicine and Biology

journal homepage: www.elsevier.com/locate/nucmedbio

A study on nitroimidazole-$^{99m}Tc(CO)_3$ complexes as hypoxia marker: Some observations towards possible improvement in in vivo efficacy

Madhava B. Mallia [a], Suresh Subramanian [a], Anupam Mathur [b], H.D. Sarma [c], Sharmila Banerjee [a,*]

[a] Isotope Applications and Radiopharmaceuticals Division, Bhabha Atomic Research Centre, Mumbai, 400085, India
[b] Medical and Biological Products Program, Board of Radiation and Isotope Technology, Mumbai, 400705, India
[c] Radiation Biology and Health Science Division, Bhabha Atomic Research Centre, Mumbai, 400085, India

ARTICLE INFO

Article history:
Received 21 January 2014
Received in revised form 27 March 2014
Accepted 14 April 2014

Keywords:
Hypoxia
Nitroimidazole
Technetium tricarbony complexes
Fibrosarcoma
Single electron reduction potential
Lipophilicity

ABSTRACT

Introduction: Hypoxia plays a negative role in the clinical management of cancer. Detection of hypoxic status of a cancer is important for selecting patients for hypoxia directed therapy. Though [^{18}F]fluoromisonidazole ([^{18}F]FMISO), a PET radiopharmaceutical, is presently being used in the clinic for the detection of hypoxia, considering the logistical advantages of ^{99m}Tc and wider availability of SPECT scanners, a radiopharmaceutical based on this isotope may find wider applicability.

Methods: Nine nitroimidazole (2-, 4- and 5-nitroimidazole) ligands were synthesized and radiolabeled using $[^{99m}Tc(CO)_3(H_2O)_3]^+$ precursor to obtain a group of complexes possessing different single electron reduction potential (SERP), overall charge and lipophilicity, the three attributes which decide the efficacy of the complex to detect hypoxic cells in vivo. The nitroimidazole-$^{99m}Tc(CO)_3$ complexes as well as [^{18}F]FMISO were evaluated in fibrosarcoma tumor bearing mice.

Results: The $^{99m}Tc(CO)_3$ complexes of nitroimidazole iminodiacetic acid (IDA) showed better tumor uptake and retention than nitroimidazole diethylenetriamine (DETA) and nitroimidazole aminoethylglycine (AEG) complexes. Tumor uptake observed with [^{18}F]FMISO was higher than any of the nitroimidazole-IDA-$^{99m}Tc(CO)_3$ complexes. However, [^{18}F]FMISO clearance from tumor was found to be faster compared to 2-nitroimidazole-IDA-$^{99m}Tc(CO)_3$ complex. Observed tumor uptake and retention of the radiotracers evaluated could be correlated to its blood clearance pattern and SERP.

Conclusions: Results of the present study indicated that uptake of the radiotracer in tumor is closely associated with its rate of clearance from blood. The study also indicated that along with SERP, clearance of radiotracer from blood (net effect of charge and lipophilicity) is a critical factor which decides the in vivo efficacy of the hypoxia detecting radiopharmaceutical.

1. Introduction

Tissue hypoxia is a condition where cells have inadequate oxygen supply leading to compromise in their biological functions. Hypoxia can occur due to several reasons including pathological conditions such as cancer, cardio/cerebrovascular disease, diabetes, infection/wound healing etc [1]. Hypoxia in cancerous lesions is a serious problem as it has direct implication on the prognosis and therapeutic outcome of the disease. The events leading to the formation of hypoxic regions in cancerous tissue are well documented [2,3].

Several experimental and clinical data had indicated a deleterious influence of hypoxia in tumor propagation, malignant progression and resistance to radiation therapy and chemotherapy [4]. Tumor hypoxia was associated with poor prognosis, especially in the case of advanced squamous cell carcinoma of cervix, advanced cancer of the uterine cervix [3,5,6], head and neck [7–9], adenocarcinoma of pancreas [10], soft tissue sarcoma etc [11]. Other potential problems associated with hypoxia have been reviewed [12]. Appropriate assessment of the hypoxic status of cancerous lesions can assist clinical oncologist to modify treatment strategy for a better clinical outcome. It can also help clinicians in selecting patients who will benefit from hypoxia directed therapy, thereby relieving other patients from the unnecessary therapeutic burden on their already deteriorated health condition.

Nitroimidazoles are widely explored compounds that can undergo oxygen dependent enzymatic reductions resulting in selective accumulation in hypoxic cells [13,14]. Several PET and SPECT agents having nitroimidazole pharmacophore have been evaluated for the detection of hypoxia [15–33]. At present, [^{18}F]FMISO is the most widely used radiopharmaceutical for the clinical assessment of tissue hypoxia [34]. Other PET radiopharmaceuticals that are clinically evaluated for imaging hypoxia, albeit to a lesser extent, include [^{18}F]FETA [17], [^{18}F]EF1 [35], [^{18}F]EF5 [36–38], [^{18}F]FAZA [39,40] and [^{18}F]FETNIM [41]. Though [^{18}F]FMISO is being used, its pharmacokinetics is far from ideal and has limitations owing to high uptake and slow clearance from non-target organs [42,43]. However, studies have established that 2 h images

* Corresponding author. Tel.: +91 22 2559 3910; fax: +91 22 2550 5345.
E-mail address: sharmila@barc.gov.in (S. Banerjee).

http://dx.doi.org/10.1016/j.nucmedbio.2014.04.103
0969-8051/

obtained using [^{18} F]FMISO clearly reflected the distribution of clinically significant hypoxic regions in the cancerous tissue [14].

Considering the favorable nuclear characteristics of ^{99m}Tc and availability of relatively larger number of SPECT scanners, a ^{99m}Tc-radiopharmaceutical which can provide clinical information equivalent to that of [^{18} F]FMISO, or superior, may find wider application. One of the possible reasons for the unsuccessful attempts to develop a radiopharmaceutical superior to [^{18} F]FMISO may be the lack of clear understanding of the optimal combination of physico-chemical parameters necessary for the radiotracer to achieve this objective. This is especially true for SPECT radiopharmaceuticals incorporating a transition metal radionuclide like ^{99m}Tc, which may form charged complexes. A charge on the complex can significantly alter its pharmacokinetics compared to neutral compounds. However, this apparent 'complication' may as well be looked upon as a tool to fine tune the pharmacokinetics of the complex in a favorable manner. To the best of our knowledge, there is no report on the comprehensive evaluation of the influence of different molecular properties that ultimately decides the overall efficacy and clinical utility of an agent indented for use in detecting tissue hypoxia.

There are evidences indicative of the role of SERP in trapping of nitroimidazole in hypoxic cells. For example, metronidazole, a 5-nitroimidazole, which has an SERP of −486 mV has been observed to undergo reduction in anaerobes but not in aerobes [44]. However, another compound misonidazole, a 2-nitroimidazole derivative having an SERP of −389 mV, has shown reduction in aerobes [45]. This indicates that the more positive the SERP value of a nitroimidazole, the better the chances of its reduction in cells having limited oxygen supply (hypoxic cells). Zhang et al. had reported an in vitro study on the effect of lipophilicity on the accumulation of 2-nitroimidazole complexes of ^{99m}Tc in CHO cells. The authors observed that anaerobic cell accumulation of the complex was related to P (partition coefficient), but within a very narrow range [46]. To the best of our knowledge in vivo evaluation of nitroimidazole ^{99m}Tc-complexes bearing different overall charge is not reported. In the present study, three series of 2-, 4- and 5-nitroimidazole ligands having tridentate ligands, viz. IDA, DETA and AEG, were envisaged and synthesized. These ligands upon radiolabeling with $[^{99m}Tc(CO)_3(H_2O)_3]^+$ precursor formed complexes with different overall charge, SERP and lipophilicity. The biological evaluation of these complexes was carried out in Swiss mice bearing fibrosarcoma tumor, and the results obtained were carefully analyzed to understand the influence of these molecular properties on overall pharmacokinetics of the radiotracer. [^{18} F]FMISO was also evaluated in the same animal model, and the results are compared with other nitroimidazole-$^{99m}Tc(CO)_3$ complexes.

2. Materials and methods

2.1. Synthesis

2.1.1. General

2-Nitroimidazole, 4-nitroimidazole and Boc-aminoethylamine were purchased from Aldrich, USA. Diethylenetriamine, 2-(tert-butoxycarbonyloxyimino)-2-phenylacetonitrile (BOC-ON), N-ethyl-diisopropylamine (DIEA), 1, 3-dibromopropane and anhydrous potassium carbonate were purchased from Fluka, Germany. All reagents were of analytical grade and used as such without additional purification unless otherwise mentioned. Silica gel plates (silica gel 60 F_{254}) used for thin layer chromatography (TLC) as well as silica gel (60–120 mesh) used for column chromatography were obtained from Merck, India. [^{18} F]FMISO was obtained from Radiation Medicine Centre, Mumbai, India. Sodium pertechnetate was eluted from ^{99}Mo/^{99m}Tc column generator using normal saline. The $[^{99m}Tc(CO)_3(H_2O)_3]^+$ precursor complex was prepared using Isolink® carbonyl kit vial obtained as a gift from Mallinckrodt Medical B. V. The HPLC analyses were performed on a JASCO PU 2080 Plus dual pump HPLC system, Japan, with a JASCO 2075 Plus tunable UV detector and a Gina Star radiometric detector system. A C18 reversed phase HiQ Sil (5 μm, 4 × 250 mm) column is used to effect separation of various components in the radioactive preparation. IR spectra were recorded on a JASCO-FT/IR-420 spectrophotometer, Japan. ^{1}H-NMR spectra were recorded either on a 300 MHz Varian VXR 300S spectrophotometer or 300 MHz Bruker AvanceII spectrophotometer. Mass spectra were recorded on a Varian 500MS Ion Trap mass spectrometer, USA. Cyclic voltammograms were recorded on a CH instrument (CHI760D), USA.

2.1.2. IDA derivatives of 2-, 4- and 5-nitroimidaole (1, 2 and 3)

The synthesis and characterization of 2-, 4- and 5-nitroimidazole-IDA derivatives were reported earlier [29].

2.1.3. DETA derivatives of 2-, 4- and 5-nitroimidaole

2.1.3.1. Synthesis of tert-butyl 2-(2-(tert-butoxycarbonyl)aminoethyl) aminoethylcarbamate (4). Selective protection of primary amine groups of diethylenetriamine was carried out using BOC-ON [47]. Diethylenetriamine (0.95 g, 9.2 mmol) in dry tetrahydrofuran (20 mL) was cooled to 0 °C in an ice bath. BOC-ON dissolved in dry tetrahydrofuran (10 mL) was added drop-wise to this solution over a period of 3 h with continuous stirring. On completion of the addition, the reaction mixture was brought to room temperature, and the stirring was continued for another 24 h. The solvent was removed using rotary evaporator. The pale yellow residue was dissolved in chloroform (100 mL) and washed with 10% NaOH (50 mL portions) till organic layer became colorless. Thereafter, organic layer was washed with brine (50 mL) and dried over anhydrous sodium sulphate. The solvent was removed using rotary evaporator, and the residue was purified by silica gel column chromatography eluting with ethyl acetate (2.34 g, 84%). R_f (methanol) = 0.70. IR (neat, cm^{-1}) 3342(w); 2976 (m); 2932(w); 2854(w); 2816(w); 1695(s); 1528(m); 1455(w); 1391(w); 1366(m); 1774(m); 1750(m); 1172(s); 781(w). ^{1}H-NMR ($CDCl_3$, δ ppm) 1.41 (s, 18H, $((CH_3)_3CO(CO)NHCH_2CH_2)_2NH$); 2.71 (t, 4H, J = 5.9 Hz, $((CH_3)_3CO(CO)NHCH_2CH_2)_2NH$); 3.19 (m, 4H, $((CH_3)_3CO(CO)NHCH_2CH_2)_2NH$). MS ($ESI^+$): 304.4 $(M + H)^+$.

2.1.3.2. Synthesis of tert-butyl 2-((2-(tert-butoxycarbonyl)aminoethyl) (3-bromopropyl)amino) ethylcarbamate (5). To compound 4 (0.55 g, 1.8 mmol) in acetonitrile (5 mL), DIEA (0.35 g, 2.7 mmol) and 1,3-dibromopropane (3.6 g, 18 mmol) were added and the mixture refluxed for 24 h with continuous stirring. The solvent was removed using rotary evaporator and further work-up was carried out following the general procedure described below. Pure compound 5 was obtained by silica gel column chromatography eluting with diethyl ether (0.35 g, 45%). R_f (diethyl ether) = 0.66, IR (neat, cm^{-1}) 3345(w); 2975 (m); 2926(w); 2850(w); 2814(w); 1694(s); 1517(m); 1455(w); 1391(w); 1365(m); 1774(m); 1749(m); 1171(s); 783(w). ^{1}H-NMR ($CDCl_3$, δ ppm) 1.45 (s, 18H, $((CH_3)_3CO(CO)NHCH_2CH_2)_2$ N-); 1.98 (quintet, 2H, J = 6.9 Hz, $BrCH_2CH_2CH_2N$-); 2.56 (t, 4H, J = 5.4 Hz, $((CH_3)_3CO(CO)NHCH_2CH_2)_2$ -N-); 2.62 (t, 2H, J = 6.9 Hz, $BrCH_2CH_2CH_2N$-); 3.19 (m, 4H, $((CH_3)_3CO(CO)NHCH_2CH_2)_2$ N-); 3.47 (t, 2H, J = 6.9 Hz, $BrCH_2CH_2CH_2N$-). MS (ESI^+): 426.4 $(M + H)^+$.

2.1.3.3. Synthesis of tert-butyl 2-((2-(tert-butoxycarbonyl)aminoethyl) (3-(2-nitro-1H-imidazol-1-yl)propyl)amino)ethylcarbamate (6). To compound 5 (0.1 g, 0.24 mmol) in acetonitrile (5 mL), DIEA (0.07 g, 0.54 mmol) and 2-nitroimidazole (0.04 g, 0.36 mmol) were added and the reaction mixture refluxed for 12 h with continuous stirring. The solvent was removed using rotary evaporator, and further work-up was carried out following the general procedure described below. Pure compound 6 was obtained by silica gel column chromatography eluting with ethyl acetate (0.1 g, 87 %). R_f (ethyl acetate) = 0.56, IR (neat, cm^{-1}) 3345 (m); 3115(w); 2972 (m); 2931 (m); 2853(w); 2818(w); 1699 (s); 1530 (s); 1471 (m); 1369 (m); 1251 (m); 1173 (s); 1122(m); 1062 (w); 972 (m); 917 (w); 859 (w); 825 (w); 745 (w); 656 (w). ^{1}H-NMR ($CDCl_3$, δ ppm) 1.43 (s, 18H, $((CH_3)_3CO(CO)NHCH_2CH_2)_2$ N-); 2.05 (quintet, 2H,

J = 7.5 Hz, 2-nitroimidazole-$CH_2CH_2CH_2N$-); 2.55 (m, 6H, $((CH_3)_3CO(CO)NHCH_2CH_2)_2NCH_2$-); 3.20 (m, 4H, $((CH_3)_3CO(CO)NHCH_2CH_2)_2$ N-); 4.46 (t, 2H, J = 7.5 Hz, 2-nitroimidazole-$CH_2CH_2CH_2N$-); 7.14 (s, 1H, 2-nitroimidazole-C5-H); 7.20 (s, 1H, 2-nitroimidazole-C4-H). MS (ESI_+): 457.4 $(M + H)_+$.

*2.1.3.4. Synthesis of tert-butyl 2-((2-(tert-butoxycarbonyl)aminoethyl) (3-(4-nitro-1H-imidazol-1-yl)propyl)amino)ethylcarbamate (**7**).* To compound 5 (0.1 g, 0.24 mmol) in acetonitrile (5 mL), DIEA (0.07 g, 0.54 mmol) and 4-nitroimidazole (0.04 g, 0.36 mmol) were added and the reaction mixture refluxed for 12 h with continuous stirring. The solvent was removed using rotary evaporator, and further work-up was carried out following the general procedure mentioned below. Pure compound **7** was obtained by silica gel column chromatography eluting with ethyl acetate (0.09 g, 79 %). R_f (ethyl acetate) = 0.41, IR (neat, cm^{-1}) 3342 (m); 3111 (w); 2976 (m); 2930 (m); 2853(w); 2819(w); 1695 (s); 1529 (s); 1475 (m); 1368 (m); 1250 (m); 1170 (s); 1121(m); 1065 (w); 972 (m); 917 (w); 858 (w); 827 (w); 744 (w); 654 (w). ^{1}H-NMR ($CDCl_3$, δ ppm) 1.44 (s, 18H, $((CH_3)_3CO(CO)NHCH_2CH_2)_2$ N-); 1.99 (quintet, 2H, J = 7.1 Hz, 4-nitroimidazole-$CH_2CH_2CH_2N$-); 2.57 (m, 6H, $((CH_3)_3CO(CO)NHCH_2CH_2)_2NCH_2$-); 3.20 (m, 4H, $((CH_3)_3CO(CO)NHCH_2CH_2)_2$ N-); 4.12 (t, 2H, J = 7.1 Hz, 4-nitroimidazole-$CH_2CH_2CH_2N$-); 7.52 (s, 1H, 4-nitroimidazole-C2-H); 7.86 (s, 1H, 4-nitroimidazole-C5-H). MS (ESI^+): 457.4 $(M + H)^+$.

2.1.3.5. Synthesis of tert-butyl-2-((2-(tert-butoxycarbonyl)aminoethyl) (3-(5-nitro-1H-imidazol-1-yl)propyl)amino)ethylcarbamate (8). Synthesis of compound 8 involved two steps.

a) Synthesis of 1-(3-bromopropyl)-5-nitro-1H-imidazole (**9**)
To 4-nitroimidazole (1 g, 9 mmol) in acetonitrile (50 mL), DIEA (1.75 g, 14 mmol) and 1, 3-dibromopropane (9 g, 45 mmol) were added and the reaction mixture stirred at room temperature for 48 h. The reaction mixture was filtered, and the filtrate was evaporated to dryness using rotary evaporator. Further work-up was carried out following the general procedure described below. Pure compound 9 was obtained by silica gel column chromatography eluting with diethyl ether (0.23 g, 11%). R_f (diethyl ether) = 0.47, IR (neat, cm^{-1}) 3114 (w); 2969 (w); 2923 (w); 1529 (s); 1371 (vs); 1121 (vs); 741 (s); 650(w). ^{1}H-NMR ($CDCl_3$, δ ppm) 2.39 (quintet, 2H, J = 6.3 Hz, 5-nitroimdazole-$CH_2CH_2CH_2$-Br); 3.36 (t, 2H, J = 6.3 Hz, 5-nitroimidazole-$CH_2CH_2CH_2Br$); 4.59 (t, 2H, J = 6.3 Hz, 5-nitroimidazole-$CH_2CH_2CH_2Br$); 7.74 (s, 1H, 5-nitroimidazole-C2-H); 8.03 (s, 1H, 5-nitroimidazole-C4-H).
b) Synthesis of tert-butyl-2-((2-(tert-butoxycarbonyl)aminoethyl) (3-(5-nitro-1H-imidazol-1-yl)propyl)amino)ethylcarbamate (8)
To compound 9 (0.07 g, 0.31 mmol) in acetonitrile (5 mL), DIEA (0.06 g, 0.47 mmol) and compound 4 (0.15 g, 0.47 mmol) were added and the reaction mixture refluxed for 12 h with continuous stirring. The solvent was removed using rotary evaporator, and further work-up was carried out following the general procedure described below. Pure compound 8 was obtained by silica gel column chromatography eluting with ethyl acetate (0.09 g, 66%). R_f (ethyl acetate) = 0.53, IR (neat, cm^{-1}) 3342 (m); 3111(w); 2976 (m); 2930 (m); 2853(w); 2819(w); 1695 (s); 1529 (s); 1475 (m); 1368 (m); 1250 (m); 1170 (s); 1121(m); 1065 (w); 972 (m); 917 (w); 858 (w); 827 (w); 744 (w); 654 (w). ^{1}H-NMR ($CDCl_3$, δ ppm) 1.44 (s, 18H, $((CH_3)_3CO(CO)NHCH_2CH_2)_2$ N-); 1.96 (quintet, 2H, J = 7.1 Hz, 5-nitroimidazole-$CH_2CH_2CH_2N$-); 2.55 (m, 6H, $((CH_3)_3CO(CO)NHCH_2CH_2)_2NCH_2CH_2CH_2$-); 3.20 (m, 4H, $((CH_3)_3CO(CO)NHCH_2CH_2)_2$ N-); 4.41 (t, 2H, J = 7.1 Hz, 5-nitroimidazole-$CH_2CH_2CH_2N$-); 7.68 (s, 1H, 5-nitroimidazole-C2-H); 8.01 (s, 1H, 5-nitroimidazole-C4-H). MS (ESI^+): 457.4 $(M + H)^+$.

2.1.3.6. Synthesis of N^1-(2-aminoethyl)-N^1-(3-(2-nitro-1H-imidazol-1-yl)propyl)ethane-1,2-diamine hydrochloride (10). Compound 6 (0.05 g, 0.11 mmol) was hydrolyzed as per the general procedure described to obtain compound 10 as hydrochloride salt. The hydrochloride salt was further purified by recrystallization from methanol/ether (0.04 g, 86%). IR (neat, cm^{-1}) 3433 (s); 3114 (w); 3013 (w); 2921 (w); 2863 (w); 1624 (m); 1531 (m); 1480 (m); 1375 (m); 1301 (w); 1268 (w); 1236 (w); 1129 (w); 1022 (w); 835 (w); 773 (w); 732 (w). ^{1}H-NMR (D_2O, δ ppm) 2.13 (quintet, 2H, J = 7.2 Hz, 2-nitroimidazole-$CH_2CH_2CH_2N$-); 2.85 (t, 2H, J = 7.2 Hz, 2-nitroimidazole-$CH_2CH_2CH_2N$-); 2.98 (t, 4H, J = 6.6 Hz, $(NH_2CH_2CH_2)_2$ N-); 3.18 (t, 4H, J = 6.6 Hz, $(NH_2CH_2CH_2)_2$ N-); 4.50 (t, 2H, J = 7.2 Hz, 2-nitroimidazole-$CH_2CH_2CH_2N$-); 7.18 (s, 1H, 2-nitroimidazole-C5-H); 7.48 (s, 1H, 2-nitroimidazole-C4-H). MS (ESI^+): 257.8 $(M + H)^+$.

2.1.3.7. Synthesis of N^1-(2-aminoethyl)-N^1-(3-(4-nitro-1H-imidazol-1-yl)propyl)ethane-1,2-diamine hydrochloride (11). Compound **7** (0.06 g, 0.13 mmol) was hydrolyzed as per the general procedure described to obtain compound 11 as hydrochloride salt. The hydrochloride salt was further purified by recrystallization from methanol/ether (0.04 g, 91%). IR (neat, cm^{-1}) 3438 (s); 3112 (w); 3009 (w); 2922 (w); 2861 (w); 1626 (m); 1530 (m); 1479 (m); 1378 (m); 1303 (w); 1267 (w); 1239 (w); 1123 (w); 1021 (w); 833 (w); 777 (w); 729 (w). ^{1}H-NMR (D_2O, δ ppm) 2.02 (quintet, 2H, J = 7.2 Hz, 4-nitroimidazole-$CH_2CH_2CH_2N$-); 2.66 (t, 2H, J = 7.2 Hz, 4-nitroimidazole-$CH_2CH_2CH_2N$-); 2.84 (t, 4H, J = 6.6 Hz, $(NH_2CH_2CH_2)_2$ N-); 3.03 (t, 4H, J = 6.6 Hz, $(NH_2CH_2CH_2)_2$ N-); 4.08 (t, 2H, J = 7.2 Hz, 4-nitroimidazole-$CH_2CH_2CH_2N$-); 7.67 (s, 1H, 4-nitroimidazole-C2-H); 8.13 (s, 1H, 4-nitroimidazole-C5-H). MS (ESI^+): 257.3 $(M + H)^+$.

2.1.3.8. Synthesis of N^1-(2-aminoethyl)-N^1-(3-(5-nitro-1H-imidazol-1-yl)propyl)ethane-1,2-diamine hydrochloride (12). Compound 8 (0.05 g, 0.11 mmol) was hydrolyzed, as per the general procedure described below, to obtain compound 12 as hydrochloride salt. The hydrochloride salt was further purified by recrystallization from methanol/ether (0.04 g, 89%). IR (neat, cm^{-1}) 3432 (s); 3110 (w); 3013 (w); 2922 (w); 2863 (w); 1625 (m); 1530 (m); 1475 (m); 1379 (m); 1301 (w); 1265 (w); 1238 (w); 1125 (w); 1017 (w); 831 (w); 771 (w); 734 (w). ^{1}H-NMR (D_2O, δ ppm) 2.22 (quintet, 2H, J = 7.2 Hz, 5-nitroimidazole-$CH_2CH_2CH_2N$-); 3.06 (t, 2H, J = 7.2 Hz, 5-nitroimidazole-$CH_2CH_2CH_2N$-); 3.18 (m, 4H, $(NH_2CH_2CH_2)_2$ N-); 3.28 (m, 4H, $(NH_2CH_2CH_2)_2$ N-); 4.54 (t, 2H, J = 7.2 Hz, 5-nitroimidazole-$CH_2CH_2CH_2N$-); 8.27 (s, 1H, 5-nitroimidazole-C2-H); 8.31(s, 1H, 5-nitroimidazole-C4-H). MS (ESI^+): 257.4 $(M + H)^+$.

2.1.3.9. Synthesis of tert-butyl-2-((tert-butoxycarbonyl)methylamino) ethylcarbamate (13). To an ice cooled solution of N-Boc-ethylenediamine (1 g, 6.28 mmol) and DIEA (0.65 g, 5.04 mmol) in acetonitrile (10 mL) tert-butylbromoacetate (0.98 g, 5.04 mmol) was added drop-wise over a period of 3 h with vigorous stirring. After the addition was completed, the reaction mixture was brought to room temperature, and the stirring continued for another 12 h. The solvent was removed using rotary evaporator, and further work-up was carried out following the general procedure mentioned below. Pure compound 13 was obtained by silica gel column chromatography eluting with ethyl acetate (0.99 g, 72%). R_f (ethyl acetate) = 0.5, IR (neat, cm^{-1}) 3343 (w); 2977 (m); 2931(w); 1730 (s); 1714 (s); 1517 (w); 1454 (w); 1392 (w); 1366 (m); 1248 (m); 1158 (s); 1045 (w); 847 (w); 780 (w). ^{1}H-NMR ($CDCl_3$, δ ppm) 1.47 (s, 18H, $(CH_3)_3CO(CO)CH_2NHCH_2CH_2NH(CO)OC(CH_3)_3$); 2.75 (t, 2H, J = 5.7 Hz, $(CH_3)_3CO(CO)CH_2NHCH_2CH_2NH(CO)OC(CH_3)_3$); 3.23 (m, 2H, $(CH_3)_3CO(CO)CH_2NHCH_2CH_2NH(CO)OC(CH_3)_3$); 3.31 (s, 2H, $(CH_3)_3CO(CO)CH_2NHCH_2CH_2NH(CO)OC(CH_3)_3$). MS ($ESI^+$): 275.4 $(M + H)^+$.

2.1.3.10. Synthesis of tert-butyl-2-(((tert-butoxycarbonyl)methyl)(3-bromopropyl)amino)ethyl carbamate (14). To compound 13 (0.68 g, 2.46 mmol) in acetonitrile (5 mL), DIEA (0.35 g, 2.7 mmol) and 1,3-dibromopropane (4.97 g, 24.6 mmol) were added and the mixture refluxed for 24 h with continuous stirring. The solvent was removed using rotary evaporator and further work-up was carried out following the general procedure mentioned below. Pure compound

14 was obtained by silica gel column chromatography eluting with chloroform (0.70 g, 72%). R_f (chloroform) = 0.55, IR (neat, cm^{-1}) 3345(w); 2975 (m); 2926(w); 2850(w); 2814(w); 1694(s); 1517 (m); 1455(w); 1391(w); 1365(m); 1774(m); 1749(m); 1171(s); 783 (w). ^{1}H-NMR ($CDCl_3$, δ ppm) 1.46 (s, 18H, $(CH_3)_3CO(CO)CH_2N(-)CH_2CH_2NH(CO)OC(CH_3)_3$); 1.99 (quintet, 2H, J = 6.6 Hz, $BrCH_2CH_2-CH_2N-$); 2.72 (t, 2H, J = 5.9 Hz, $-(CO)CH_2N(-)CH_2CH_2NH-$); 2.75 (t, 2H, J = 6.6 Hz, $BrCH_2CH_2CH_2N-$); 3.18 (m, 2H, $-(CO)CH_2N(-)CH_2-CH_2NH-$); 3.22 (s, 2H, $-(CO)CH_2N(-)CH_2CH_2NH-$); 3.48 (t, 2H, J = 6.6 Hz, $BrCH_2CH_2CH_2N-$). MS (ESI^+): 395.4 $(M + H)^+$.

2.1.3.11. Synthesis of tert-butyl 2-(((tert-butoxycarbonyl)methyl)(3-(2-nitro-1H-imidazol-1-yl)propyl)amino)ethyl carbamate (15). To compound 14 (0.42 g, 1.06 mmol) in acetonitrile (5 mL), DIEA (0.23 g, 1.75 mmol) and 2-nitroimidazole (0.13 g, 1.1 mmol) were added and the reaction mixture refluxed for 12 h with continuous stirring. The solvent was removed using rotary evaporator, and further work-up was carried out following the general procedure described below. Pure compound 15 was obtained by silica gel column chromatography eluting with ethyl acetate (0.40 g, 89%). R_f (ethyl acetate) = 0.8, IR (neat, cm^{-1}) 3413 (w); 3116 (w); 2976 (m); 2928 (m); 2855 (w); 1714 (s); 1538 (m); 1487 (m); 1455 (w); 1365 (s); 1250 (w); 1159 (s); 1074 (w); 835 (w); 784 (w). ^{1}H-NMR ($CDCl_3$, δ ppm) 1.45 (s, 9H, $(CH_3)_3CO(CO)CH_2N(-)CH_2CH_2NH(CO)OC(CH_3)_3$); 1.48 (s, 9H, $(CH_3)_3CO(CO)CH_2N(-)CH_2CH_2-NH(CO)OC(CH_3)_3$); 1.98 (quintet, 2H, J = 6.6 Hz, 2-nitroimidazole-$CH_2CH_2CH_2N-$); 2.63 (t, 2H, J = 6.3 Hz, $-(CO)CH_2N(-)CH_2CH_2NH-$); 2.75 (t, 2H, J = 6.6 Hz, 2-nitroimidazole-$CH_2CH_2CH_2N-$); 3.22 (m, 4H, $-(CO)CH_2N(-)CH_2CH_2NH-$); 4.54 (t, 2H, J = 6.6 Hz, 2-nitroimidazole-$CH_2CH_2CH_2N-$); 7.12 (s, 1H, 2-nitroimidazole-C5-H); 7.27 (s, 1H, 2-nitroimidazole-C4-H). MS (ESI^+): 450.4 $(M + Na)^+$.

2.1.3.12. Synthesis of tert-butyl-2-(((tert-butoxycarbonyl)methyl)(3-(4-nitro-1H-imidazol-1-yl)propyl)amino)ethyl carbamate (16). To compound 14 (0.15 g, 0.38 mmol) in acetonitrile (5 mL), DIEA (0.06 g, 0.46 mmol) and 4-nitroimidazole (0.05 g, 0.42 mmol) were added and the reaction mixture refluxed for 12 h with continuous stirring. The solvent was removed using rotary evaporator, and further work-up was carried out following the general procedure mentioned below. Pure compound 16 was obtained by silica gel column chromatography eluting with diethyl ether (0.12 g, 72%). R_f (diethyl ether) = 0.3, IR (neat, cm^{-1}) 3404 (w); 3127 (w); 2976 (w); 2919 (w); 2849 (w); 1731 (w); 1698 (s); 1541 (m); 1513 (w); 1455 (w); 1366 (w); 1337 (w); 1287 (w); 1247 (w); 1156 (s); 975 (w); 854 (w). ^{1}H-NMR ($CDCl_3$, δ ppm) 1.41 (s, 9H, $(CH_3)_3CO(CO)CH_2N(-)CH_2CH_2NH(CO)OC(CH_3)_3$); 1.43 (s, 9H, $(CH_3)_3CO(CO)CH_2N(-)CH_2-CH_2NH(CO)OC(CH_3)_3$); 1.98 (quintet, 2H, J = 6.6 Hz, 4-nitroimidazole-$CH_2CH_2CH_2N-$); 2.65 (m, 4H, $-CH_2CH_2CH_2N(-)CH_2CH_2NH-$); 3.15 (m, 4H, $-(CO)CH_2N(-)CH_2CH_2NH-$); 4.19 (t, 2H, J = 6.6 Hz, 4-nitroimidazole-$CH_2CH_2CH_2N-$); 7.50 (s, 1H, 4-nitroimidazole-C2-H); 7.84 (s, 1H, 4-nitroimidazole-C5-H). MS (ESI^+): 450.4 $(M + Na)^+$.

2.1.3.13. Synthesis of tert-butyl-2-(((tert-butoxycarbonyl)methyl)(3-(5-nitro-1H-imidazol-1-yl)propyl)amino)ethyl carbamate (17). To compound 9 (0.07 g, 0.31 mmol) in acetonitrile (5 mL), DIEA (0.6 g, 0.47 mmol) and compound 13 (0.13 g, 0.47 mmol) were added and the reaction mixture refluxed for 12 h with continuous stirring. The solvent was removed using rotary evaporator, and further work-up was carried out following the general procedure mentioned below. Pure compound 17 was obtained by silica gel column chromatography eluting with diethyl ether (0.09 g, 70%). R_f (diethyl ether) = 0.55, IR (neat, cm^{-1}) 3402 (w); 3109 (w); 2976 (m); 2930 (w); 2860 (w); 1713 (s); 1529 (m); 1474 (m); 1368 (s); 1248 (m); 1157 (s); 1145 (w); 854 (w); 826 (w); 744 (w). ^{1}H-NMR ($CDCl_3$, δ ppm) 1.45 (s, 9H, $(CH_3)_3CO(CO)CH_2N(-)CH_2CH_2NH(CO)OC(CH_3)_3$); 1.48 (s, 9H, $(CH_3)_3CO(CO)CH_2N(-)CH_2CH_2-NH(CO)OC(CH_3)_3$); 1.94 (quintet, 2H, J = 6.4 Hz, 5-nitroimidazole-$CH_2CH_2CH_2N-$); 2.61 (t, 2H, J = 6.4 Hz, 5-nitroimidazole-$CH_2CH_2CH_2-N-$); 2.68 (t, 2H, J = 6.2 Hz, $-CH_2N(-)CH_2CH_2NH-$); 3.21 (m, 4H, $-CH_2N(-)CH_2CH_2NH-$); 4.50 (t, 2H, J = 6.4 Hz, 5-nitroimidazole-$CH_2CH_2CH_2N-$); 7.72 (s, 1H, 5-nitroimidazole-C2-H); 8.01 (s, 1H, 5-nitroimidazole-C4-H). MS (ESI^+): 450.5 $(M + Na)^+$.

2.1.3.14. Synthesis of 2-(N-(2-aminoethyl)-N-(3-(2-nitro-1H-imidazol-1-yl)propyl)amino)acetic acid hydrochloride (18). Compound 15 (0.1 g, 0.23 mmol) was hydrolyzed as per the general procedure described to obtain compound 18 as hydrochloride salt. The hydrochloride salt was further purified by recrystallization from methanol/ether (0.07 g, 90%). IR (KBr, cm^{-1}) 3430 (m); 3206 (m); 3130 (w); 2990 (w); 2928 (w); 2679 (w); 2596 (w); 1688 (s); 1504 (w); 1487 (m); 1468 (w); 1357 (s); 1163 (m); 963 (m); 834 (m); 753 (w). ^{1}H-NMR (D_2O, δ ppm) 2.27 (quintet, 2H, J = 7.9 Hz, 2-nitroimidazole-$CH_2CH_2CH_2N-$); 3.37 (m, 4H, 2-nitroimidazole-$CH_2-CH_2CH_2N(-)(CH_2CH_2-)$); 3.49 (m, 2H, 2-nitroimidazole-$CH_2CH_2CH_2N(-)(CH_2CH_2NH_2)$); 3.84 (s, 2H, 2-nitroimidazole-$CH_2CH_2CH_2N(-)CH_2-COOH$); 4.45 (t, 2H, J = 7.9 Hz, 2-nitroimidazole-$CH_2CH_2CH_2N(-)CH_2COOH$); 7.09 (s, 1H, 2-nitroimidazole-C5-H); 7.37 (s, 1H, 2-nitroimidazole-C4-H). MS (ESI^+): 271.3 $(M)^+$.

2.1.3.15. Synthesis of 2-(N-(2-aminoethyl)-N-(3-(4-nitro-1H-imidazol-1-yl)propyl)amino)acetic acid hydrochloride (19). Compound 16 (0.05 g, 0.15 mmol) was hydrolyzed as per the general procedure described to obtain compound 19 as hydrochloride salt. The hydrochloride salt was further purified by recrystallization from methanol/ether (0.04 g, 84%). IR (KBr, cm^{-1}) 3432 (m); 3200 (m); 3131 (w); 2994 (w); 2924 (w); 2675 (w); 2596 (w); 1689 (s); 1506 (w); 1484 (m); 1470 (w); 1358 (s); 1165 (m); 964 (m); 837 (m); 755 (w). ^{1}H-NMR (D_2O, δ ppm) 2.39 (quintet, 2H, J = 4.8 Hz, 4-nitroimidazole-$CH_2CH_2CH_2N-$); 3.40 (m, 4H, 4-nitroimidazole-$CH_2-CH_2CH_2N(-)(CH_2CH_2NH_2)$); 3.62 (t, 2H, J = 7.5 Hz, $-CH_2CH_2CH_2N(-)(CH_2CH_2NH_2)$); 4.03 (s, 2H, $-CH_2CH_2CH_2N(-)CH_2COOH$); 4.27 (t, 2H, J = 4.8 Hz, 4-nitroimidazole-$CH_2CH_2CH_2N-$); 7.79 (s, 1H, 4-nitroimidazole-C2-H); 8.24 (s, 1H, 4-nitroimidazole-C5-H).

2.1.3.16. Synthesis of 2-(N-(2-aminoethyl)-N-(3-(5-nitro-1H-imidazol-1-yl)propyl)amino)acetic acid hydrochloride (20). Compound 17 (0.05 g, 0.15 mmol) was hydrolyzed as per the general procedure described to obtain compound 20 as hydrochloride salt. The hydrochloride salt was further purified by recrystallization from methanol/ether (0.05 g, 90%). IR (KBr, cm^{-1}) 3435 (m); 3201 (m); 3133 (w); 2991 (w); 2931 (w); 2675 (w); 2599 (w); 1689 (s); 1500 (w); 1489 (m); 1465 (w); 1360 (s); 1164 (m); 961 (m); 835 (m); 756 (w). ^{1}H-NMR (D_2O, δ ppm) 2.41 (quintet, 2H, J = 4.8 Hz, 5-nitroimidazole-$CH_2CH_2CH_2N-$); 3.42 (m, 4H, 5-nitroimidazole-$CH_2CH_2CH_2N(-)(CH_2CH_2NH_2)$); 3.60 (t, 2H, J = 7.5 Hz, $-CH_2CH_2CH_2N(-)(CH_2CH_2NH_2)$); 4.10 (s, 2H, $-CH_2CH_2CH_2N(-)CH_2COOH$); 4.45 (t, 2H, J = 4.8 Hz, 5-nitroimidazole-$CH_2CH_2CH_2N-$); 8.28 (s, 1H, 5-nitroimidazole-C2-H); 8.35 (s, 1H, 5-nitroimidazole-C4-H). MS (ESI^+): 271.6 $(M)^+$.

2.1.4. General work up procedure for compounds 5-9 and 13-17

The residue obtained after the removal of the reaction solvent was dissolved in chloroform (30 mL) and washed with water (15 mL × 3) followed by brine (30 mL). The organic phase was dried over anhydrous sodium sulphate, concentrated and purified by silica gel column chromatography using appropriate solvent.

2.1.5. General procedure for the hydrolysis of Boc- and tert-butyl ester groups in compound 10–12 and 18–20

Respective compound was dissolved in minimum volume of methanol and added to 6 N HCl (~5 mL). The reaction mixture was stirred at room temperature for 12 h. The solvent was removed using rotary evaporator at 40 °C to obtain corresponding hydrochloride salt.

2.1.5.1. Preparation of $Re(CO)_3$ complex of 12 (21). Compound 12 (0.08 g, 0.2 mmol) was dissolved in water (5 mL), and the pH of the solution was adjusted to 6 with 0.1 N NaOH. To this solution bis (tetraethylammonium)-*fac*-tribromotricarbonylrhenate (0.15 g, 0.2 mmol), prepared following a reported procedure [48], was added, and the mixture was heated at 50 °C for 12 h. The precipitate formed was removed by filtration. To the filtrate excess of solid $NaBF_4$ was added to obtain precipitate of target complex 21 as tetrafluoroborate salt (0.04 g, 32%). IR (KBr, cm^{-1}) 3130 (m); 2984 (m); 2950 (m); 2692 (w); 2016 (vs); 1878 (vs); 1646 (s); 1491 (w); 1395 (m); 1337 (m); 1288 (w); 1183 (w); 1133 (w). ^{1}H-NMR (D_2O, δ ppm) 2.39 (quintet, 2H, J = 7.9 Hz, 5-nitroimidazole-$CH_2\underline{CH_2}CH_2$N-); 2.89 and 3.00 (m, 4H, $(H_2NCH_2\underline{CH_2})_2NCH_2CH_2CH_2$-); 3.15 (m, 2H, $((H_2NCH_2$-$CH_2)_2N\underline{CH_2}CH_2CH_2$-); 3.44 and 3.90 (m, 4H, $(H_2N\underline{CH_2}CH_2)_2NCH_2CH_2$-$CH_2$N-); 4.45 (t, 2H, J = 7.9 Hz, 5-nitroimidazole-$\underline{CH_2}CH_2CH_2$N-); 7.99 (s, 1H, 5-nitroimidazole-C2-H); 8.11 (s, 1H, 5-nitroimidazole-C4-H). MS (ESI^+): 528.2 $(M + H)^+$.

2.1.5.2. Preparation of $Re(CO)_3$ complex of 19 (22). Complex 22 was prepared following similar procedure described for complex 21, from compound 19 (0.07 g, 0.18 mmol) and bis(tetraethylammonium)-*fac*-tribromotricarbonylrhenate (0.14 g, 0.18 mmol) in water (5 mL, pH = 6). The mixture was heated at 50 °C for 12 h. The precipitate obtained was filtered off, and the filtrate was evaporated to obtain crude product. IR (KBr, cm^{-1}) 3132 (m); 2984 (m); 2953 (m); 2695 (w); 2017 (vs); 1878 (vs); 1646 (s); 1492 (w); 1395 (m); 1339 (m); 1287 (w); 1182 (w); 1133 (w). ^{1}H-NMR (D_2O, δ ppm) 1.91 (quintet, 2H, J = 4.8 Hz, 4-nitroimidazole-$CH_2\underline{CH_2}CH_2$N-); 2.38 and 2.58 (m, 2H, -$CH_2CH_2CH_2$N(-)($\underline{CH_2}CH_2NH_2$)); 3.00 (t, 2H, 4-nitroimidazole-$CH_2CH_2\underline{CH_2}$N(-)(CH_2CH_2-$\underline{NH_2}$)); 3.43 and 4.00 (m, 2H, -$CH_2CH_2CH_2$N(-)($\underline{CH_2}CH_2NH_2$)); 3.81 (m, 2H, -$CH_2CH_2CH_2$N(-)$\underline{CH_2}$COOH); 4.12 (t, 2H, 4-nitroimidazole-$\underline{CH_2}CH_2$-CH_2N-); 7.60 (s, 1H, 4-nitroimidazole-C2-H); 8.06 (s, 1H, 4-nitroimidazole-C5-H). MS (ESI^+): 566.2 $(M + H)^+$.

2.2. Radiolabeling

2.2.1. Preparation of $[^{99m}Tc(CO)_3(H_2O)_3]^+$ precursor complex

The procedure involved the addition of 1 mL of freshly eluted $Na^{99m}TcO_4$ from $^{99}Mo/^{99m}TcO_4^-$ alumina column generator to the Isolink® kit vial and heating the vial at 95 °C for 20 min. After cooling and re-equilibrating to atmospheric pressure, the pH of the reaction mixture was adjusted to 7 using 1:3 mixture of 0.5 M phosphate buffer (pH 7.4):1 N HCl.

2.2.2. General procedure for the preparation of different nitroimidazole-$^{99m}Tc(CO)_3$ complexes

About 100 μL of freshly prepared $[^{99m}Tc(CO)_3(H_2O)_3]^+$ precursor complex was added to 900 μL of 10^{-3} M solution of the respective ligand in phosphate buffer (pH 7.4) and incubated for 30 min in a 70 °C water bath. The reaction mixture was then cooled to room temperature and analyzed by HPLC.

2.3. Physicochemical studies

2.3.1. HPLC

The radiochemical purity of the $[^{99m}Tc(CO)_3(H_2O)_3]^+$ precursor complex as well as different nitroimidazole-$^{99m}Tc(CO)_3$ complexes were assessed by HPLC with a C18 reversed phase column. About 15 μL of the test solution (~0.37 MBq) was injected into the column, and elution was monitored by observing the radioactivity profile. Aqueous 0.05 M triethylammonium phosphate (TEAP) buffer, pH = 2.5, (solvent A) and methanol (solvent B) were used as the mobile phase. Both the solvents were filtered through 0.22 μ filter. The elution started with 100% A from 0 to 6 min. At 6 min the eluent switched to 75% A and 25% B and at 9 min to 66% A and 34% B followed by a linear gradient 66% A/34% B to 100% B from 9 to 20 min. Up to 30 min the eluent remained at 100% B before switching back to the initial condition. Flow rate was maintained at 1 mL/min.

2.3.2. Partition coefficient ($LogP_{o/w}$)

About 100 μL of the labeled compound was mixed with 0.9 mL of water and 1 mL of n-octanol on a vortex mixer for about 3 min and then centrifuged at 3500 g for 5 min to effect clear separation of the two layers. About 0.8 mL of the octanol layer was withdrawn, and equal volume of water was added. The mixture was vortexed again and then centrifuged as described above. Equal aliquots in triplicate were withdrawn from n-octanol, and aqueous layer and radioactivity associated with each layer was determined in a NaI(Tl) counter. The partition coefficient was calculated using the equation: $LogP_{o/w}$ = Log[(counts in n-octanol layer)/(counts in aqueous layer)].

2.3.3. In vitro serum stability

About 50 μL of the labeled compound (~0.37 MBq) was added to 500 μL of human serum, and this mixture was incubated at 37 °C for 3 hours. An aliquot of 100 μL was drawn after 3 h, and an equal volume of ethanol was mixed to precipitate the serum proteins. The mixtures were centrifuged, and the supernatants were analyzed by HPLC to assess stability of the complex in serum.

2.3.4. Electrochemical studies

Cyclic voltammogram of nitroimidazole ligands and complex was carried out using a glassy carbon working electrode, platinum counter electrode and an Ag/Ag^+ as reference electrode, following a procedure previously reported by Lei Mei et al [49]. Solutions for analysis were prepared in anhydrous DMF just prior to the studies and contained ~5 mM concentration of analyte and tetrabutylammonium perchlorate (TBAP) (0.1 mol/mL). Ferrocene was used as a reference standard for which the one electron reduction process occurs at $E_{1/2}$ = 0.47 V in DMF (containing 0.1 mol/mL of TBAP) versus standard calomel electrode [50]. Before recording the voltammograms, the test solution was thoroughly purged with high purity argon gas to remove any tracers of dissolved oxygen. Scan rate was maintained at 50 mV/s.

2.4. In vivo studies

All procedures performed herein were in strict compliance with the national laws governing the conduct of animal experiments. Solid tumor models were developed in Swiss mice by implantation of HSDM1C1 murine fibrosarcoma. About 10^6 cells in 100 μL volume per animal were injected subcutaneously on the dorsum. The tumors were allowed to grow till they were approximately 10 mm in diameter after which the animals were used for the experiment. For the biodistribution studies, the radioactive preparation (~3.7 MBq per animal in 100 μL volume) was administered intravenously through the lateral tail vein. Individual sets of animals (n = 3) were utilized for studying the biodistribution at different time points (30 min, 60 min, and 180 min). At the end of the respective time periods, the animals were sacrificed and the relevant organs excised for measurement of retained activity. The organs were weighed, and the activity associated with them was measured in a flat-bed type NaI (Tl) counter with suitable energy window for $^{99m}Tc/^{18}$ F. The activity retained in each organ/tissue was expressed as a per cent value of the injected dose per gram (%ID/g).

2.4.1. Determination of stability of nitroimidazole complexes in vivo

The blood collected from the tumor bearing animal at 3 h p.i., after measuring the activity associated with it, was allowed to clot, and the serum is separated. Serum proteins are then precipitated using ethanol and separated by centrifugation. Supernatant is then analyzed by HPLC.

2.5. Statistical analysis

Statistical analysis of relevant data was performed by one-way analysis of variance (ANOVA). Confidence level of 95% ($p < 0.05$) was taken for statistical significance.

3. Results and discussion

To study the influence of molecular properties such as SERP, lipophilicity and overall charge on pharmacokinetics, a series of nitroimidazole complexes were prepared and evaluated. The ligands envisaged to achieve this objective are shown in Fig. 1. The synthesis of the ligands [Fig. 1(a)] for the preparation of 2-, 4- and 5-nitroimidazole-IDA-$^{99m}Tc(CO)_3$ complexes has been reported earlier [29]. Syntheses of other ligands [Fig. 1(b) & (c)] are described in the experimental section.

There is substantial evidence to correlate the SERP of nitroimidazole to their efficiency to get reduced in hypoxic cells [51–54]. The SERP of a nitroimidazole depends on the position of the nitro group as well as the nature and position of other substituent in the imidazole ring. Peter Wardman had compiled and published the SERP of a number of nitroimidazole derivatives. Typical values of SERP of unsubstituted 2-, 4- and 5-nitroimidazole is −418 mV, −527 mV and −450 mV, respectively, with respect to standard hydrogen electrode in aqueous solution [55]. The nitroimidazole ligands synthesized in the present study had one of the three tridentate ligands viz. IDA, DETA or AEG linked to N1-nitrogen atom of the imidazole ring through a propyl spacer (Fig. 1). Adams et al. had observed that functional groups that are separated by two or more carbon–carbon bonds from the nitroimidazole ring had minimal effect on its SERP [52,54]. However, in the present work, limited cyclic voltametric studies were carried out to confirm the applicability of Adam's observations to the ligands being evaluated. Generally, SERP of nitroimidazole is determined by pulse radiolysis of its aqueous solutions. However, Breccia et al. [56] had shown a linear correlation existing between the SERP values of nitroimidazoles compounds measured by pulse radiolysis and by cyclic voltammetry in aprotic solvent such as dimethylformamide (DMF). Table 1 shows the SERP values of 2- and 4-nitroimidazole, and its derivatives measured by cyclic voltammetry in anhydrous DMF. SERP of 5-nitroimidazole could not be carried out due to its unavailability; however, two of its derivatives were analyzed. Typical cyclic voltammogram obtained for 2- & 4-nitroimidazole is shown in Fig. 2.

The first cathodic peak represents the reduction of nitro group to nitro-radical anion which is designated as the SERP of the nitroimidazole/nitroimidazole ligand [57]. From Table 1, it could be observed that the SERP value of the 2-nitroimidazole actually varies upon introduction or modification of the side chain attached to N1 nitrogen atom of the nitroimidazole. However, the variation is within a narrow range from the SERP of the unsubstitued 2-nitroimidazole (−0.92 ± 0.12 V) which broadly confirms Adam's observations. Similar trend could be observed with 4-nitroimidazole and its derivatives. Thus, it could be assumed that variation in SERP due to the synthetic modifications would be within an acceptable range for different 2-nitroimidazole (1, 10, 18), 4-nitroimidazole (2, 11, 19), and 5-nitroimidazole (3, 12, 20) derivatives and the trend observed in the SERP value of bare 2-, 4- and 5-nitroimidazole (−418 mV, −527 mV, −450 mV with respect to standard hydrogen electrode in aqueous solution, respectively) will also be valid for their derivatives in aqueous solution. With this set of nine ligands, corresponding $^{99m}Tc(CO)_3$ complexes with different SERP could be prepared.

The nitroimidazole ligands (10-12 and 18-20) were radiolabeled using $[^{99m}Tc(CO)_3(H_2O)_3]^+$ precursor complex to obtain corresponding $^{99m}Tc(CO)_3$ complexes. The RCP as well as typical specific activity of various nitroimidazole complexes is shown in Table 2. All nitroimidazole-$^{99m}Tc(CO)_3$ complexes appeared as a single peak, the only other radiochemical impurity being the un-complexed $[^{99m}Tc(CO)_3(H_2O)_3]^+$ precursor complex. Hence, the radiochemical yield of various nitroimidazole complexes is same as its RCP.

The $[^{99m}Tc(CO)_3(H_2O)_3]^+$ precursor introduced by Alberto et al. [58] permitted the preparation of complexes with different overall charge using ligands having appropriate donor groups. The ligands used in the present study, viz. IDA, DETA and AEG, were carefully chosen considering this ability of $[^{99m}Tc(CO)_3(H_2O)_3]^+$ precursor complex. The three substitution labile water molecule in $[^{99m}Tc(CO)_3(H_2O)_3]^+$ precursor facilitated the formation of stable pseudo-octahedral complexes with tridentate ligands. The IDA ligands (1, 2, 3) upon radiolabeling using $[^{99m}Tc(CO)_3(H_2O)_3]^+$ precursor formed $^{99m}Tc(CO)_3$-complexes with an overall negative charge [59]. Similarly, DETA ligands (10, 11, 12) formed $^{99m}Tc(CO)_3$ complexes with overall positive charge, and AEG ligands (18, 19, 20) formed neutral complexes when radiolabeled using $[^{99m}Tc(CO)_3(H_2O)_3]^+$ precursor complex [60]. All complexes were analyzed by HPLC. The HPLC retention time observed with different nitroimidazole complexes was tabulated in Table 2.

Due to the structural diversity, the lipophilicity of nitroimidazole-$^{99m}Tc(CO)_3$ complexes is expected to be different. The octanol/water partition coefficient ($LogP_{o/w}$), an indicator of lipophilicity, of various nitroimidazole complexes were determined following a reported procedure [61] and are summarized in Table 2. It could be seen that nitroimidazole-AEG-$^{99m}Tc(CO)_3$ complexes were least lipophilic followed by nitroimidazole-DETA-$^{99m}Tc(CO)_3$ complexes

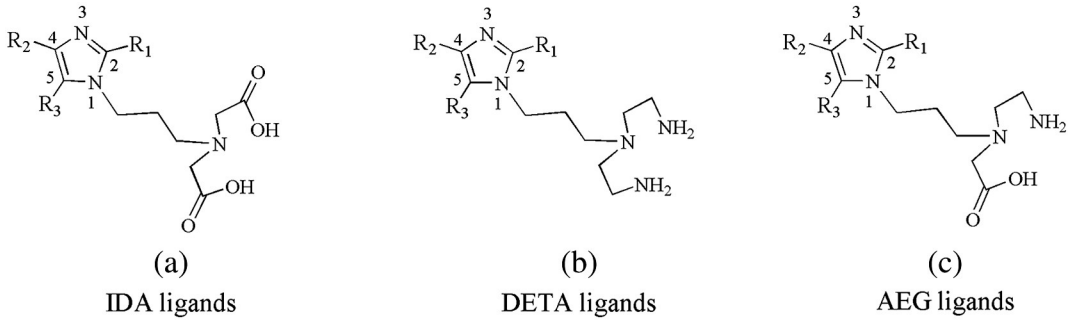

$R_1 = NO_2$; R_2, R_3 = H --- 2-nitroimidazole-IDA (**1**), 2-nitroimidazole-DETA (**10**), 2-nitroimidazole-AEG (**18**)
$R_2 = NO_2$; R_1, R_3 = H --- 4-nitroimidazole-IDA (**2**), 4-nitroimidazole-DETA (**11**), 4-nitroimidazole-AEG (**19**)
$R_3 = NO_2$; R_1, R_2 = H --- 5-nitroimidazole-IDA (**3**), 5-nitroimidazole-DETA (**12**), 5-nitroimidazole-AEG (**20**)

Fig. 1. Structure of various ligands used in the present study.

Table 1
Reduction potential different nitroimidazole derivatives and $Re(CO)_3$ complex of 2-nitroimidazole-IDA derivative.

	Single electron reduction potential (V)		
	2-Nitroimidazole	4-Nitroimidazole	5-Nitroimidazole
Unsubstituted	−0.92	−1.23	-
Bromide derivative	−0.80	−1.30	−1.17 (9)
Tridentate derivative	−1.01 (*tert*-butyl ester derivative)	−1.26 (8)	−1.11 (16)
$Re(CO)_3$ complex	−0.63, −0.89	-	-

and nitroimidazole-IDA-$^{99m}Tc(CO)_3$ complexes. Incubation of various nitroimidazole-$^{99m}Tc(CO)_3$ complexes in human serum at 37 °C did not show any signs of decomposition during the period of study (3 h).

To elucidate the mode of binding of the ligand with $^{99m}Tc(CO)_3$ core in the complex, corresponding $Re(CO)_3$ complex of 5-nitroimidazole-DETA (12) as well as 4-nitroimidazole-AEG (19) were synthesized in macroscopic level as representatives of the respective nitroimidazole ligand series. The preparation and characterization of 2-nitroimidazole-IDA-$Re(CO)_3$ complex was reported earlier [29]. The $Re(CO)_3$-analogues of 12 and 19 were prepared as described in the experimental section. HPLC analysis showed that elution profiles of 5-nitroimidazole-DETA-$Re(CO)_3$ complex and 4-nitroimidazole-AEG-$Re(CO)_3$ complex matched with the corresponding $^{99m}Tc(CO)_3$ complexes prepared at no-carrier-added (nca) level (Table 2). This indicated the formation of similar types of complexes both at the nca level as well as at macroscopic levels. Observation of $(M + H)^+$ ion peak at m/z 528.2 and $(M + H)^+$ ion peak at m/z 566.2 provided additional evidence for the formation of 5-nitroimidazole-DETA-$Re(CO)_3$ and 4-nitroimidazole-AEG-$Re(CO)_3$ complexes respectively. The ^{1}H-NMR spectrum of 5-nitroimidazole-DETA-$Re(CO)_3$ showed complex splitting pattern typical of AB spin systems corresponding to the 8 methylene protons of the diethylenetriamine moiety which indicated the tridentate coordination between the three nitrogen atoms of diethylenetriamine and $Re(CO)_3$ metal core [62]. Similar, complicated, splitting pattern in the ^{1}H-NMR spectrum of 4-nitroimidazole-AEG-$Re(CO)_3$ together with the disappearance of singlet at 4.03 δ ppm corresponding to the two methylene protons of acetic acid moiety, indicated tridentate coordination between AEG and $Re(CO)_3$ core.

As already mentioned the voltammograms of various nitroimidazole derivatives showed variation in their SERP within a narrow range compared to the corresponding unsubstituted nitroimidazole. To see the variation in SERP of the nitroimidazole ligand upon complexation with tricarbonyl core, the voltammogram of $Re(CO)_3$ complex of 2-nitroimidazole-IDA was recorded. The voltammograms of 2-nitroimidazole-IDA-$Re(CO)_3$ complex showed two reduction waves at

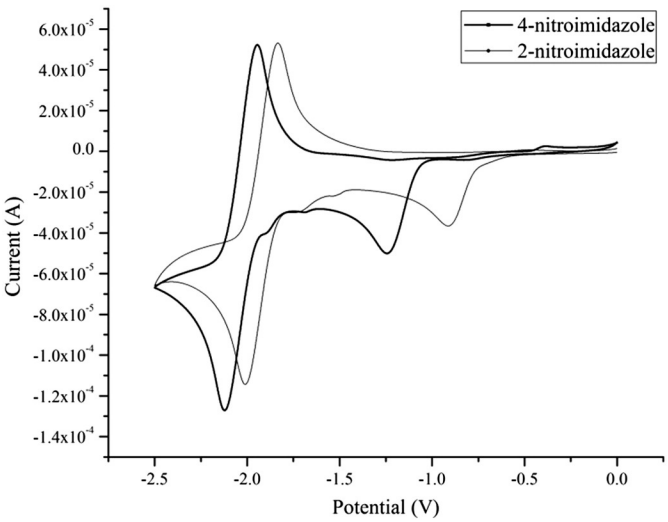

Fig. 2. Voltammogram unsubstituted 2- and 4-nitroimidazole.

−0.63 V and −0.89 V which is similar to the observation made by Lei Mei et al. [49]. These two reduction waves must be due to the nitroimidazole moiety, since IDA-$Re(CO)_3$ complex did not showed any reduction peak in the region from 0 V to −2.5 V in anhydrous DMF. The origin of this double reduction wave pattern in the voltammogram of 2-nitroimidazole-IDA-$Re(CO)_3$ complex is not investigated. However, it is pertinent to note that both reduction waves (−0.63 V and −0.89 V) appeared at a more positive value than the SERP of 2-nitroimidazole (−0.92 V) indicating that the ability of the 2-nitroimidazole to undergo reduction in hypoxic cells has not deteriorated upon complexation with metal tricarbonyl core.

The biodistribution studies of DETA and AEG $^{99m}Tc(CO)_3$ complexes of 2-, 4- and 5- nitroimidazole was carried out in Swiss mice bearing fibrosarcoma tumor. Markus et al. [63] had reported a study on the determination of hypoxic status of 12 different types of tumors growing in mice using Eppendorf histograph, including RIF-1, which is a fibrosarcoma tumor. Their study showed a median pO_2 of 2.7 mmHg in RIF-1 fibrosarcoma tumor grown at the back of the C3H mice, clearly indicating its hypoxic nature. We presumed that fibrosarcoma tumor used in the present study will also be sufficiently hypoxic. However, since hypoxic status of the tumor was not determined, biodistribution of clinically used hypoxia detecting radiopharmaceutical [^{18} F]FMISO was also carried out in same tumor bearing animal so that in vivo performance of the various nitroimidazole-$^{99m}Tc(CO)_3$ complexes reported in the present study can be directly compared.

The tumor activity observed with different nitroimidazole-$^{99m}Tc(CO)_3$ complexes and [^{18} F]FMISO at different time points are shown in Table 3. For comparison, results of the biological evaluation of 2-, 4- and 5-nitroimidazole-IDA-$^{99m}Tc(CO)_3$ complexes, reported earlier [29], are also included. It is worth mentioning here that uptake of [^{18} F]FMISO in tumor could be seen as an indirect evidence for the hypoxic nature of fibrosarcoma tumor used in the present study.

At 30 min p.i. small differences were observed in tumor uptake among different nitroimidazole-IDA-$^{99m}Tc(CO)_3$ complexes and nitroimidazole-AEG-$^{99m}Tc(CO)_3$ complexes. However, these differences were not significant ($p > 0.05$) for the 4- and 5-nitroimidazole complexes of either groups. Among the three nitroimidazole-DETA-$^{99m}Tc(CO)_3$ complexes, no significant differences were observed in tumor uptake at 30 min p.i. At the same reference time, [^{18} F]FMISO showed significantly higher uptake in tumor [4.65 (0.86) %ID/g] than any of the nitroimidazole-$^{99m}Tc(CO)_3$ complexes evaluated in the present study. These observations could not be explained considering the SERP of nitroimidazole alone. Also, Zhang et al. had studied a number of 2-nitroimidazole ^{99m}Tc-complexes with P values ranging from 0.0002 to 5 ($LogP_{o/w}$ ranging from −3.7 to 0.70), and they have observed that variation in anaerobic cell accumulation of the radiotracer in vitro is within a very narrow range [46]. Since lipophilicity values of different nitroimidazole-$^{99m}Tc(CO)_3$ complexes being evaluated in the present study are within this range, the observed variation in tumor uptake at 30 min p.i. may not be due to the small variation in their lipophilicity either. However, a possible explanation could be obtained considering the blood clearance pattern of respective radiotracers (Table 3). A radiotracer that clears slowly from blood enables it to distribute better in tumor by passive diffusion along the concentration gradient established between blood and the intracellular environment of the tumor. Considering the

Table 2
HPLC retention time, $LogP_{o/w}$, radiochemical purity and typical specific activity of different nitroimidazole complexes.

	2-Nitroimidazole				4-Nitroimidazole				5-Nitroimidazole			
	Retention time (min)	$LogP_{o/w}$	% RCP (HPLC, n = 3)	Specific activity (μCi/μmol of ligand, n = 3)[#]	Retention time (min)	$LogP_{o/w}$	% RCP (HPLC, n = 3)	Specific activity (μCi/μmol of ligand, n = 3)[#]	Retention time (min)	$LogP_{o/w}$	% RCP (HPLC, n = 3)	Specific activity (μCi/μmol of ligand, n = 3)[#]
IDA-$^{99m}Tc(CO)_3$ complex	20.9	0.48	96 ± 1	106.7 ± 1.1	19.8	0.43	97 ± 1	107.8 ± 1.1	19.9	0.39	96.3 ± 0.8	107.0 ± 0.6
IDA-$Re(CO)_3$ complex	20.3	-	-	-	-	-	-	-	-	-	-	-
DETA-$^{99m}Tc(CO)_3$ complex	15.3	0.28	95.3 ± 1.2	105.9 ± 1.3	16.7	0.17	94 ± 0.6	104.8 ± 0.6	16.1	0.15	94.7 ± 0.6	105.2 ± 0.6
DETA-$Re(CO)_3$ complex	-	-	-	-	-	-	-	-	15.9	-	-	-
AEG-$^{99m}Tc(CO)_3$ complex	14.2	0.06	95.6 ± 1.2	106.3 ± 1.3	18.2	−0.43	95.7 ± 1.5	106.3 ± 1.7	18	−0.53	95.7 ± 1.5	106.3 ± 1.7
AEG-$Re(CO)_3$ complex	-	-	-	-	18.1	-	-	-	-	-	-	-

[#] Specific activity at the end of preparation. Specific activity not corrected for ^{99m}Tc decay during preparation.

deteriorated vasculature that could be expected in a tumor, the radiotracer may have to traverse a longer diffusion path to distribute across the entire tumor mass. This requires the concentration gradient to hold for sufficient period of time. Fast clearance of activity from the blood results in early reversal of concentration gradient which may affect the distribution of the radiotracer in the tumor mass. Reversal of the concentration gradient will also initiate the clearance of unreduced radiotracer from the tumor, thereby significantly decreasing its residence time in tumor. The observed tumor uptake of different radiotracers at 30 min p.i. may be the result of these two effects happening in varying proportions. For [^{18} F]FMISO, about 4% ID/g of activity was still present in blood at 30 min p.i., whereas, only 1% or less of blood activity was observed for DETA and AEG-$^{99m}Tc(CO)_3$ complexes at the same reference time. Consequently, [^{18} F]FMISO showed higher tumor uptake compared to the latter group of complexes. Low blood activity of DETA and AEG-$^{99m}Tc(CO)_3$ complexes could be attributed to their faster clearance from blood, mainly through hepatobiliary route, which is evident from the presence of significant levels of activity in liver and intestines as early as 30 min p.i. (Tables 4 and 5). The three nitroimidazole-IDA-$^{99m}Tc(CO)_3$ complexes cleared more slowly than DETA and AEG-$^{99m}Tc(CO)_3$ complexes. Accordingly, they showed relatively higher tumor uptake than DETA and AEG-$^{99m}Tc(CO)_3$ complexes, but lower than [^{18} F]FMISO.

Tumor uptake and retention of nitroimidazole complexes are being strongly associated with their blood clearance pattern; it assumes significance to ascertain whether the activity retained in blood is due to the intact nitroimidazole complex or its metabolites. This is done by analyzing the blood sample collected from the tumor bearing animal at 3 h p.i. The HPLC analysis showed that more than 85% of the activity in blood is due to the intact nitroimidazole complex. This analysis was carried out only for nitroimidazole-IDA complexes which clear relatively slowly from blood.

It is pertinent to note that, while tumor uptake observed with [^{18} F]FMISO as well as different DETA and AEG-$^{99m}Tc(CO)_3$ complexes at 30 min p.i. were similar or slightly higher than their respective activity in blood (expressed in %ID/g), the tumor uptake observed with nitroimidazole-IDA$^{99m}Tc(CO)_3$ complexes were lower, despite having higher lipophilicity and blood activity than DETA and AEG-$^{99m}Tc(CO)_3$ complexes. Pauletti et al. had reported similar observations where tripeptides with comparable size diffuse across the cell membrane in a charge dependent manner, the order of diffusion rates being negative < positive ≤ neutral [64]. Possibly the negative charge on the compound may be hindering its smooth diffusion across the negatively charged cell membrane.

At 60 min p.i., [^{18} F]FMISO as well as other nitroimidazole-$^{99m}Tc(CO)_3$ complexes, except 5-nitroimidazole-IDA-$^{99m}Tc(CO)_3$ complex, showed a decrease in tumor activity observed at 30 min p.i. The decrease was shallow for [^{18} F]FMISO and three nitroimidazole-IDA-$^{99m}Tc(CO)_3$ complexes, whereas for nitroimidazole-DETA and nitroimidazole-AEG-$^{99m}Tc(CO)_3$ complexes the decrease was sharp (Table 3). The tumor associated activity observed with different nitroimidazole radiotracers at 60 min p.i. cleared slowly, indicating that it could be due to the radiotracer reduced and trapped in hypoxic tumor cells. The possibility that observed tumor activity is due to the non-specific binding of the radiotracer was ruled out considering the steadily decreasing radioactivity level in muscles with time (Tables 4 & 5). The decrease in tumor associated activity between 30 and 60 min p.i. for different radiotracers could be attributed to the clearance of unbound nitroimidazole radiotracer from the tumor. The difference in the tumor retention showed by different nitroimidazole-$^{99m}Tc(CO)_3$ complexes and [^{18} F]FMISO at 60 min p.i. could be attributed to their respective SERP and residence time in tumor. The ease of nitroimidazole radical anion formation in the cell depends on the SERP of the nitroimidazole, wherein a nitroimidazole with more

Table 3
Activity of different nitroimidazole-$^{99m}Tc(CO)_3$ complexes and [^{18} F]FMISO observed in tumor and blood at different time points (n = 3).

		$^{99m}Tc(CO)_3$ complex									[^{18}F]FMISO
		2-Nitroimidazole			4-Nitroimidazole			5-Nitroimidazole			
		IDA	DETA	AEG	IDA	DETA	AEG	IDA	DETA	AEG	
Tumor %ID/g (s.d)[#]	30 min	0.97 (0.06)	1.05 (0.25)	1.33 (0.28)	0.56 (0.17)	1.10 (0.07)	1.01 (0.11)	0.45 (0.09)	1.07 (0.09)	0.91 (0.03)	4.65 (0.86)
	60 min	0.71 (0.01)	0.31 (0.04)	0.38 (0.03)	0.40 (0.06)	0.35 (0.03)	0.32 (0.05)	0.47 (0.02)	0.33 (0.05)	0.34 (0.04)	3.70 (0.09)
	180 min	0.66 (0.07)	0.24 (0.06)	0.30 (0.04)	0.13 (0.02)	0.27 (0.15)	0.25 (0.03)	0.36 (0.04)	0.30 (0.04)	0.29 (0.05)	2.04 (0.14)
Blood %ID/g (s.d)[#]	30 min	3.04 (0.39)	1.93 (0.38)	1.15 (0.16)	0.54 (0.11)	0.64 (0.10)	0.85 (0.06)	0.90 (0.07)	0.92 (0.03)	0.97 (0.09)	3.95 (0.31)
	60 min	1.82 (0.09)	1.28 (0.19)	1.04 (0.04)	0.44 (0.02)	0.45 (0.02)	0.43 (0.02)	0.44 (0.05)	0.38 (0.04)	0.40 (0.02)	2.38 (0.42)
	180 min	1.09 (0.06)	0.77 (0.25)	0.74 (0.05)	0.28 (0.08)	0.18 (0.02)	0.20 (0.02)	0.17 (0.01)	0.21 (0.03)	0.24 (0.02)	0.53 (0.07)

[#] %ID/g – Percentage injected dose per gram; s.d. – standard deviation.

Table 4
Distribution of nitroimidazole-DETA-$^{99m}Tc(CO)_3$ complexes in various organs at different time points (n = 3).

Organ	DETA-$^{99m}Tc(CO)_3$ complex %ID/g (s.d.)[#]								
	30 min			60 min			180 min		
	2-Nitro imidazole	4-Nitro imidazole	5-Nitro imidazole	2-Nitro imidazole	4-Nitro imidazole	5-Nitro imidazole	2-Nitro imidazole	4-Nitro imidazole	5-Nitro imidazole
Liver	14.65 (0.68)	27.92 (3.69)	27.67 (1.50)	13.08 (1.34)	24.14 (4.82)	21.98 (2.65)	8.98 (1.69)	9.70 (1.76)	10.09 (2.01)
Intestines	27.55 (0.85)	12.90 (0.36)	14.88 (4.21)	23.93 (3.97)	13.51 (2.39)	20.25 (4.06)	27.06 (2.11)	13.96 (0.70)	21.07 (4.04)
Kidney	8.48 (1.87)	8.13 (0.64)	7.68 (1.39)	5.84 (0.45)	5.97 (0.18)	7.12 (0.20)	4.08 (0.98)	4.34 (0.23)	6.13 (0.63)
Heart	0.77 (0.02)	0.42 (0.11)	0.33 (0.08)	0.53 (0.10)	0.24 (0.01)	0.19 (0.02)	0.46 (0.13)	0.28 (0.07)	0.20 (0.03)
Lungs	1.33 (0.15)	1.32 (0.21)	1.12 (0.12)	1.33 (0.24)	1.05 (0.18)	1.02 (0.04)	0.83 (0.17)	0.64 (0.13)	0.44 (0.06)
Spleen	0.79 (0.11)	1.13 (0.04)	0.63 (0.07)	0.52 (0.09)	0.72 (0.08)	0.55 (0.04)	0.42 (0.05)	0.46 (0.08)	0.42 (0.03)
Muscle	0.32 (0.07)	0.16 (0.01)	0.11 (0.01)	0.13 (0.02)	0.09 (0.01)	0.07 (0.01)	0.13 (0.03)	0.05 (0)	0.05 (0.01)
Bone	0.21 (0.06)	0.09 (0.03)	0.07 (0.01)	0.06 (0.02)	0.08 (0.03)	0.05 (0.02)	0.06 (0.02)	0.08 (0.01)	0.04 (0.01)

[#] %ID/g – Percentage injected dose per gram; s.d. – standard deviation.

positive SERP form radical anions quicker than the nitroimidazole with lower SERP. However, owing to small levels of molecular oxygen present in viable hypoxic cells, the nitroimidazole radiotracer may have to undergo several futile reduction–oxidation cycles, between the radical anion of the complex and the parent complex, before it undergoes further reduction and trapping. It implies that, even nitroimidazoles with a favorable SERP need to spend adequate time in hypoxic cells to undergo reduction and trapping. Therefore, fast clearance of nitroimidazole radiotracer from blood could significantly reduce its tumor residence time, and hence, its reduction in hypoxic cells, despite having favorable SERP. This may be the reason for the lower tumor retention showed by different DETA- and AEG-$^{99m}Tc(CO)_3$ complexes of 2-nitroimidazole.

The tumor activity observed with [^{18} F]FMISO and the three nitroimidazole-IDA-$^{99m}Tc(CO)_3$ complexes at 60 min p.i. could be correlated to their respective tumor residence time and SERP. [^{18} F] FMISO, which had higher tumor residence time, by virtue of its slower clearance from blood, and a more favorable SERP (−389 mV with respect to standard hydrogen electrode in aqueous solution [55]), showed highest retention in tumor, followed by 2-, 5- and 4-nitroimidazole-$^{99m}Tc(CO)_3$ complexes, respectively. The exact cause for slow blood clearance of IDA-$^{99m}Tc(CO)_3$ complexes is not clear. However, it has been reported that molecules with overall negative charge showed relatively higher binding to serum as compared to positively charged and neutral molecules. Also, molecules with higher lipophilicity are known to show higher serum binding leading to slower clearance from blood [65,66].

Retrospectively, negative influence of fast blood clearance of nitroimidazole radiotracers on their tumor uptake and subsequent retention could be obtained from literature. BMS181321 and BRU59-21 are two 2-nitroimidazole-based ^{99m}Tc-complexes which showed oxygen dependent accumulation in hypoxic cells in vitro as well as in vivo. Though a direct comparison between different nitroimidazole-$^{99m}Tc(CO)_3$ complexes evaluated in the present work, BMS181321 and BRU59-21 would be inappropriate due to the difference in tumor models used, the trends in their distribution may be analyzed. Upon intravenous administration of BMS181321 in mice bearing KHT tumor, tumor uptake of 1.91 ± 0.29 %ID/g was observed at 10 min p.i., which then decreased to 0.73 ± 0.22 at 1 h p.i. and 0.53 ± 0.26 at 4 h p.i. BMS181321 is a highly lipophilic complex ($LogP_{o/w}$ = ~40) and cleared slowly from blood (~5 %ID/g at 10 min p.i. and ~2 %ID/g at 4 h p.i.). BRU59-21 ($LogP_{o/w}$ = ~11) was a similar 2-nitroimidazole complex designed to overcome the problems associated with the high lipophilicity of BMS181321. This complex, which was also evaluated in mice bearing KTH tumor, showed very fast clearance from blood (1.56 ± 0.43 %ID/g at 10 min p.i., 0.53 ± 0.05 %ID/g at 1 h p.i. and 0.40 ± 0.08 %ID/g at 4 h p.i.) which had a significant effect on the activity retained in tumor (0.73 ± 0.22 %ID/g at 10 min p.i., 0.37 ± 0.04 %ID/g at 1 h p.i. and 0.31 ± 0.18 %ID/g at 4 h p.i.) [67,68]. Similarly, [^{18} F]FAZA which clears relatively faster from blood showed lower uptake in tumor than [^{18} F]FMISO in Walker 256 rat carcinosarcoma tumor bearing animal model [15].

Although the tumor activity retained by different nitroimidazole radiotracers at 60 min p.i. cleared slowly, the rate of clearance was highest for [^{18} F]FMISO (~44 % ID/g cleared at 180 min p.i.) compared to other nitroimidazole-$^{99m}Tc(CO)_3$ complexes (~8-20 %ID/g cleared at 180 min p.i.). [^{18} F]FAZA has also been reported with rate of clearance similar to [^{18} F]FMISO between 60 and 180 min (~53 % ID/g cleared) [15]. There is still some ambiguity on the fate of reduction products of nitroimidazoles in hypoxic cells. Though nitroimidazole adducts such as misonidazole-glutathione and metronidazole-DNA are reported [69,70], a more widely accepted view is the formation of less permeable reduction products, that cleared slowly from hypoxic cells, rather than the formation of covalently bound macro-

Table 5
Distribution of nitroimidazole-AEG-$^{99m}Tc(CO)_3$ complexes in various organs at different time points (n = 3).

Organ	AEG-$^{99m}Tc(CO)_3$ complex %ID/g (s.d.)[#]								
	30 min			60 min			180 min		
	2-Nitro imidazole	4-Nitro imidazole	5-Nitro imidazole	2-Nitro imidazole	4-Nitro imidazole	5-Nitro imidazole	2-Nitro imidazole	4-Nitro imidazole	5-Nitro imidazole
Liver	13.02 (2.96)	13.45 (2.03)	14.84 (1.54)	2.59 (4.83)	11.10 (2.21)	11.24 (3.35)	6.19 (1.36)	7.23 (1.93)	5.51 (2.03)
Intestines	8.24 (4.88)	19.53 (3.44)	20.46 (1.90)	22.21 (2.05)	25.22 (1.38)	23.60 (2.64)	22.85 (3.80)	29.12 (2.87)	31.19 (1.99)
Kidney	4.02 (1.94)	5.24 (0.88)	7.11 (0.82)	2.77 (1.06)	1.21 (0.19)	0.89 (0.10)	0.82 (0.30)	0.70 (0.05)	0.53 (0.08)
Heart	0.58 (0.23)	0.70 (0.05)	0.32 (0.06)	0.19 (0.05)	0.69 (0.04)	0.27 (0.06)	0.06 (0.02)	0.33 (0.05)	0.11 (0.02)
Lungs	0.86 (0.41)	1.19 (0.34)	1.21 (0.24)	0.43 (0.11)	0.53 (0.11)	0.52 (0.05)	0.27 (0.09)	0.20 (0.03)	0.11 (0.03)
Spleen	0.67 (0.05)	0.45 (0.08)	0.23 (0.09)	0.19 (0.08)	0.14 (0.03)	0.11 (0.02)	0.28 (0.08)	0.12 (0.02)	0.09 (0.01)
Muscle	0.32 (0.18)	0.51 (0.03)	0.59 (0.06)	0.10 (0.03)	0.30 (0.02)	0.24 (0.04)	0.09 (0.01)	0.12 (0.01)	0.12 (0.04)
Bone	0.25 (0.06)	0.09 (0.03)	0.06 (0.01)	0.06 (0.02)	0.05 (0.01)	0.04 (0.02)	0.06 (0.02)	0.03 (0.01)	0.03 (0.01)

[#] %ID/g – Percentage injected dose per gram; s.d. – standard deviation.

moleculear adducts [16]. A probable cause for the slower clearance of tumor activity of various nitroimidazole-$^{99m}Tc(CO)_3$ complexes compared to [^{18} F]FMISO between 60 min p.i. and 180 min p.i. could be that the reduction products of nitroimidazole-$^{99m}Tc(CO)_3$ complexes are less permeable than that of [^{18} F]FMISO. Whatever be the actual reasons, slower clearance of nitroimidazole-$^{99m}Tc(CO)_3$ complexes could be an advantage, since the imaging can be delayed to obtain better contrast between the hypoxic regions and the background which may not be feasible with short lived isotopes such as ^{18} F.

Though slow blood clearance could help in increasing the tumor residence time of the radiotracer, thereby increasing the chances of nitroimidazole radiotracer reduction in hypoxic tumor cells, too slow blood clearance may result in poor target to background ratio. For nitroimidazole-IDA-$^{99m}Tc(CO)_3$ complexes, significant blood activity even at 3 h p.i. resulted in poor tumor to blood ratio (TBR) [Table 6]. On the other hand, nitroimiazole-DETA-$^{99m}Tc(CO)_3$ and nitroimidazole-AEG-$^{99m}Tc(CO)_3$ complexes cleared very fast from blood resulting in low retention in tumor, but better TBR (between 1 to 1.9). It is interesting to note, at this juncture, that blood clearance of [^{18} F]FMISO was gradual, approximately following a path between the two extremes, the slow blood clearance of IDA-$^{99m}Tc(CO)_3$ complexes on one side and fast blood clearance by DETA- and AEG-$^{99m}Tc(CO)_3$ complexes on the other. While initial high blood activity of [^{18} F]FMISO facilitated hypoxia specific reduction, by providing sufficient residence time for [^{18} F]FMISO in tumor, subsequent clearance from blood gradually increased TBR.

The in vivo distribution observed with different nitroimidazole-DETA-$^{99m}Tc(CO)_3$ complexes and nitroimidazole-AEG-$^{99m}Tc(CO)_3$ complexes in tumor bearing Swiss mice is shown in Tables 4 and 5, respectively. All the nitroimidazole-$^{99m}Tc(CO)_3$ complexes evaluated in the present study cleared majorly through the hepatobiliary route.

While majority of publications on agents for targeting tumor hypoxia discusses their synthesis and biological evaluation, present study has made an attempt to understand the factors deciding the efficacy of the radiotracer in vivo. Analysis of the biodistribution results reported herein suggests that along with SERP and optimal blood clearance of the nitroimidazole radiotracer is an important factor that decides the usefulness of a nitroimidazole radiopharmaceutical for the detection of hypoxia. The significance of tumor residence time of the radiotracer, which depends on the clearance of the radiotracer from blood, is probably less illustrated before. Fast clearance of the radiotracer from blood, which generally leads to high TBR, is considered to be a virtue for diagnostic radiopharmaceuticals [67,68,21]. However, this can lead to low uptake of radiotracer in tumor, which could result in some of the clinically significant hypoxic regions going undetected. Hence, improving TBR by designing molecules that clear faster from blood, probably, should not be the criteria while developing new nitroimidazole radiopharmaceuticals for detecting hypoxia. Finding of this study may be helpful while designing next generation radiopharmaceuticals for the detection of tumor hypoxia.

Table 6
Tumor to blood ratio obtained with different nitroimidazole- $^{99m}Tc(CO)_3$ complexes and [^{18} F]FMISO at various time points.

		Tumor to blood ratio		
		30 min	60 min	180 min
IDA-$^{99m}Tc(CO)_3$ complex	2-nitroimidazole	0.32 (0.04)	0.39 (0.01)	0.61 (0.09)
	4-nitroimidazole	0.29 (0.03)	0.31 (0.05)	0.18 (0.04)
	5-nitroimidazole	0.40 (0.11)	0.45 (0.04)	0.49 (0.09)
DETA-$^{99m}Tc(CO)_3$ complex	2-nitroimidazole	1.94 (0.09)	0.71 (0.08)	0.84 (0.05)
	4-nitroimidazole	1.72 (0.17)	0.78 (0.06)	1.51 (0.27)
	5-nitroimidazole	1.26 (0.15)	0.78 (0.13)	1.48 (0.15)
AEG-$^{99m}Tc(CO)_3$ complex	2-nitroimidazole	1.49 (0.41)	0.86 (0.04)	1.78 (0.34)
	4-nitroimidazole	1.09 (0.13)	0.86 (0.15)	1.06 (0.14)
	5-nitroimidazole	0.95 (0.08)	0.85 (0.12)	1.26 (0.35)
	[^{18} F]FMISO	1.17 (0.18)	1.58 (0.25)	3.85 (0.23)

4. Conclusions

The $^{99m}Tc(CO)_3$ chemistry provides a tool for the manipulation of blood clearance of nitroimidazole radiotracers. It could be noted that the tridentate ligands that coordinate with the $^{99m}Tc(CO)_3$ core had a significant effect on the blood clearance of the resultant nitroimidazole complexes. While the IDA-$^{99m}Tc(CO)_3$ complexes showed slow blood clearance, the DETA- and AEG-$^{99m}Tc(CO)_3$ complexes cleared very fast from blood. By incorporating appropriate hydrophilic groups in nitroimidazole-IDA-$^{99m}Tc(CO)_3$ complexes, it may be possible to adequately improve its blood clearance to obtain better TBR without significantly affecting the tumor uptake. Similarly, by sufficiently increasing the lipophilicity, for example by increasing the length of the linker, blood clearance of DETA- and AEG-$^{99m}Tc(CO)_3$ complexes may be slowed down to improve tumor uptake while retaining favorable TBR. However, it is difficult to predict the rate of blood clearance that would provide optimum tumor residence time for a given nitroimidazole radiotracer to undergo adequate reduction in tumor, to enable unambiguous detection of all clinically relevant hypoxic regions, at the same time produce acceptable values of TBR. Modifying a nitroimidazole ^{99m}Tc-radiotracer to mimic the blood clearance pattern of [^{18} F]FMISO could be an interesting idea to explore. If a nitroimidazole-$^{99m}Tc(CO)_3$ complex, that significantly accumulates as well as detects all clinically relevant hypoxic regions in a tumor, could be developed, the option of using the corresponding $^{186/188}Re(CO)_3$ analogue to deliver direct therapeutic dose to the hypoxic tumor tissues could be explored.

Acknowledgment

The authors acknowledge Mr. Suvendu Sen, student of M.Sc., IIT, Roorkee and Ms. Hina Parveen Shaikh, student of M.Sc., SIES College of Arts, Science and Commerce, Mumbai, who helped in the synthesis. Authors also acknowledge the staff of Radiochemicals Section, Isotope Application and Radiopharmaceuticals Division, for providing ^{99}Mo for our work. Authors also thank Dr. Manoj Sharma, Fuel Chemistry Division, BARC, for helping to carryout cyclic voltametry studies.

References

[1] Wiebe LI, Machulla HJ. Hypoxia: an introduction. In: Machulla HJ, editor. Imaging Hypoxia. Netherlands: Kluwer Academic Publishers; 1999. p. 1–18.
[2] Hockel M, Vaupel P. Tumor hypoxia: definitions and current clinical, biologic and molecular aspects. J Natl Cancer Inst 2001;93:266–76.
[3] Mees G, Dierckx R, Vangestel C, Van de Wiele C. Molecular imaging of hypoxia with radiolabelled agents. Eur J Nucl Med Mol Imaging 2009;36:1674–86.
[4] Gray LH, Conger AD, Ebert M. The concentration of oxygen dissolved in tissues at the time of irradiation as a factor in radiotherapy. Br J Radiol 1953;26:638–48.
[5] Höckel M, Schlenger K, Aral B, Mitze M, Schäffer U, Vaupel P. Association between tumor hypoxia and malignant progression. Cancer Res 1996;56:4509–15.
[6] Fyles AW, Milosevic M, Wong R, Kavanagh MC, Pintilie M, Sun A, et al. Oxygenation predicts radiation response and survival in patients with cervix cancer. Radiother Oncol 1998;48:149–56.
[7] Nordsmark M, Overgaard M, Overgaard J. Pretreatment oxygenation predicts radiation response in advanced squamous cell carcinoma of the head and neck. Radiother Oncol 1996;41(1):31–9.
[8] Brizel DM, Sibley GS, Prosnitz LR, Scher RL, Dewhirst MW. Tumor hypoxia adversely affects the prognosis of carcinoma of the head and neck. Int J Radiat Oncol Biol Phys 1997;38(2):285–9.
[9] Nordsmark M, Bentzen SM, Rudat V, Brizel D, Lartigau E, Stadler P, et al. Prognostic value of tumor oxygenation in 397 head and neck tumors after primary radiation therapy. An international multi-center study. Radiother Oncol 2005;77(1):18–24.
[10] Duffy JP, Eibl G, Reber HA, Hines OJ. Influence of hypoxia and neoangiogenesis on the growth of pancreatic cancer. Mol Cancer 2003;2:12.
[11] Brizel DM, Scully SP, Harrelson JM, Layfield LJ, Bean JM, Prosnitz LR, et al. Tumor oxygenation predicts for the likelihood of distant metastases in human soft tissue sarcoma. Cancer Res 1996;56(5):941–3.
[12] McKeown SR, Cowen RL, Williams KJ. Bioreductive drugs: from concept to clinic. Clin Oncol 2007;19(6):427–42.

[13] Tocher JH. Reductive activation of nitroheterocyclic compounds. Gen Pharmacol 1997;28(4):485–7.
[14] Krohn KA, Link JM, Mason RP. Molecular imaging of hypoxia. J Nucl Med 2008 (Suppl 2):129S–48S.
[15] Grunbaum Z, Freauff SJ, Krohn KA, Wilbur DS, Magee S, Rasey JS. Synthesis and characterization of congeners of misonidazole for imaging hypoxia. J Nucl Med 1987;28(1):68–75.
[16] Nunn A, Linder K, Strauss HW. Nitroimidazoles and imaging hypoxia. Eur J Nucl Med 1995;22(3):265–80.
[17] Rasey JS, Hofstrand PD, Chin LK, Tewson TJ. Characterization of [^{18} F]fluoroetanidazole, a new radiopharmaceutical for detecting tumor hypoxia. J Nucl Med 1999;40(6):1072–9.
[18] Lewis JS, McCarthy DW, McCarthy TJ, Fujibayashi Y, Welch MJ. Evaluation of 64Cu-ATSM in vitro and in vivo in a hypoxic tumor model. J Nucl Med 1999;40(1): 177–83.
[19] Evans SM, Kachur AV, Shiue CY, Hustinx R, Jenkins WT, Shive GG, et al. Noninvasive detection of tumor hypoxia using the 2-nitroimidazole [^{18} F]EF1. J Nucl Med 2000;41(2):327–36.
[20] Ballinger JR. Imaging hypoxia in tumors. Semin Nucl Med 2001;31(4):321–9.
[21] Sorger D, Patt M, Kumar P, Wiebe LI, Barthel H, Seese A, et al. [^{18} F] Fluoroazomycinarabinofuranoside (^{18}FAZA) and [^{18} F]Fluoromisonidazole (^{18}FMISO): a comparative study of their selective uptake in hypoxic cells and PET imaging in experimental rat tumors. Nucl Med Biol 2003;30(3):317–26.
[22] Tatum JL, Kelloff GJ, Gillies RJ, Arbeit JM, Brown JM, Chao KS, et al. Hypoxia: importance in tumor biology, noninvasive measurement by imaging, and value of its measurement in the management of cancer therapy. Int J Radiat Biol 2006;82(10): 699–757.
[23] Komar G, Seppänen M, Eskola O, Lindholm P, Grönroos TJ, Forsback S, et al. 18 F-EF5: a new PET tracer for imaging hypoxia in head and neck cancer. J Nucl Med 2008;49(12):1944–51.
[24] Mallia MB, Banerjee S, Venkatesh M. Technetium-99 m labelled molecules for hypoxia imaging. Technetium-99 m Radiopharmaceuticals: Status and Trends. Vienna: IAEA; 2009 295–316.
[25] Bonnitcha PD, Bayly SR, Theobald MB, Betts HM, Lewis JS, Dilworth JR. Nitroimidazole conjugates of bis(thiosemicarbazonato) 64Cu(II) - Potential combination agents for the PET imaging of hypoxia. J Inorg Biochem 2010;104(2):126–35.
[26] Zha Z, Zhu L, Liu Y, Du F, Gan H, Qiao J, et al. Synthesis and evaluation of two novel 2-nitroimidazole derivatives as potential PET radioligands for tumor imaging. Nucl Med Biol 2011;38(4):501–8.
[27] Mathur A, Mallia MB, Banerjee S, Sarma HD, Pillai MR. Preparation and evaluation of a ^{99m}TcN-PNP complex of sanazole analogue for detecting tumor hypoxia. Bioorg Med Chem Lett 2013;23(5):1394–7.
[28] Mallia MB, Kumar C, Mathur A, Sarma HD, Banerjee S. On the structural modification of 2-nitroimidazole-(99 m)Tc(CO)(3) complex, a hypoxia marker, for improving in vivo pharmacokinetics. Nucl Med Biol 2012;39(8):1236–42.
[29] Mallia MB, Subramanian S, Mathur A, Sarma HD, Venkatesh M, Banerjee S. Synthesis and evaluation of 2-, 4- and 5-substituted nitroimidazole-iminodiacetic acid-^{99m}Tc(CO)$_3$ complexes to target hypoxic tumors. J Label Compd Radiopharm 2010;53:535–42.
[30] Sakr TM, El-Safoury DM, Awad GA, Motaleb MA. Biodistribution of 99mTc-sunitinib as a potential radiotracer for tumor hypoxia imaging. J Labelled Comp Radiopharm 2013;56(8):392–5.
[31] Shan L. (99 m)Tc-2-[Bis-(2-mercaptoethyl)]aminoethanethiol-4-isocyano-N-[2-(2-methyl-5-nitro-1H-imidazol-1-yl)ethyl]butanamide. Molecular Imaging and Contrast Agent Database (MICAD) [Internet]; 2012. Available from http://www.ncbi.nlm.nih.gov/books/NBK98638/.
[32] Giglio J, Fernández S, Pietzsch HJ, Dematteis S, Moreno M, Pacheco JP, et al. Synthesis, in vitro and in vivo characterization of novel 99mTc-'4 + 1'-labeled 5-nitroimidazole derivatives as potential agents for imaging hypoxia. Nucl Med Biol 2012;39(5):679–86.
[33] Huang H, Zhou H, Li Z, Wang X, Chu T. Effect of a second nitroimidazole redox centre on the accumulation of a hypoxia marker: synthesis and in vitro evaluation of 99mTc-labeled bisnitroimidazole propylene amine oxime complexes. Bioorg Med Chem Lett 2012;22(1):172–7.
[34] Lee ST, Scott AM. Hypoxia positron emission tomography imaging with 18 F-fluoro misonidazole. Semin Nucl Med 2007;37(6):451–61.
[35] Kachur AV, Dolbier Jr WR, Evans SM, Shiue CY, Shiue GG, Skov KA, et al. Synthesis of new hypoxia markers EF1 and [^{18} F]-EF1. Appl Radiat Isot 1999;51:643–50.
[36] Couturier O, Luxen A, Chatal JC, Vuillez JP, Rigo P, Hustinx R. Fluorinated tracers for imaging cancer with positron emission tomography. Eur J Nucl Med Mol Imaging 2004;31:1182–206.
[37] Dolbier Jr WR, Li AR, Koch CJ, Shiue CY, Kachur AV. [^{18} F]EF5, a marker for PET detection of hypoxia: synthesis of precursor and a new fluorination procedure. Appl Radiat Isot 2001;54:73–80.
[38] Mahy P, De Bast M, Gillart J, Labar D, Grégoire V. Detection of tumour hypoxia: comparison between EF5 adducts and [^{18} F]EF3 uptake on an individual mouse tumour basis. Eur J Nucl Med Mol Imaging 2006;33:553–6.
[39] Piert M, Machulla HJ, Picchio M, Reischl G, Ziegler S, Kumar P, et al. Hypoxia-specific tumor imaging with ^{18} F-fluoroazomycin arabinoside. J Nucl Med 2005;46(1):106–13.
[40] Reischl G, Dorow DS, Cullinane C, Katsifis A, Roselt P, Binns D, et al. Imaging of hypoxia with [^{124}I]IAZA in comparison with [^{18} F]FMISO and [^{18} F]FAZA-first small animal PET results. J Pharm Pharm Sci 2007;10(2):203–11.
[41] Yang DJ, Wallace S, Cherif A, Li C, Gretzer MB, Kim EE, et al. Development of F-18-labeled fluoroerythronitromidazole as a PET agent for imaging tumor hypoxia. Radiology 1995;194(3):795–800.
[42] Koh WJ, Rasey JS, Evans ML, Grierson JR, Lewellen TK, Graham MM, et al. Imaging of hypoxia in human tumors with [F-18]fluoromisonidazole. Int J Radiat Oncol Biol Phys 1992;22(1):199–212.
[43] Valk PE, Mathis CA, Prados MD, Gilbert JC, Budinger TF. Hypoxia in human gilomas: demonstration by PET with fluorine-18-misonidazole. J Nucl Med 1992;33(12):2133–7.
[44] Edwards DI. Nitroimidazole drugs-action and resistance mechanisms. 1. Mechanism of action. J Antimicrob Chemother 1993;31:9–20.
[45] Brown JM. Hypoxic cell radiosensitizers: where next? Int J Radiat Oncol Biol Phys 1989;16:987–93.
[46] Zhang X. Su Zi-Fen, Ballinger JR, Rauth AM, Pollak A, Thornback JR. Targeting hypoxia in tumors using 2-nitroimidazoles with peptidic chelators for Technetium-99 m: Effect of lipophilicity. Bioconjug Chem 2000;11:401–7.
[47] Itoh M, Hagiwara D, Kamiya T. A new tert-butyloxycarbonylating reagent, 2-tert-butyloxycarbonyloxyimino-2-phenyl acetonitrile. Tetrahedron Lett 1975;16(49): 4393–4.
[48] Alberto R, Schibli R, Schubiger PA, Abram U, Kaden TA. Reactions with the technetium and rhenium carbonyl complexes $(NEt_4)_2[MX_3(CO)_3]$. Synthesis and structure of $[Tc(CN\text{-}Bu^t)_3(CO)_3](NO_3)$ and $(NEt_4)[Tc_2(\mu\text{-}SCH_2CH_2OH)_3(CO)_6]$. Polyhedron 1996;15:1079–89.
[49] Mei L, Wang Y, Chu T. 99mTc/Re complexes bearing bisnitroimidazole or mononitroimidazole as potential bioreductive markers for tumor: synthesis, physicochemical characterization and biological evaluation. Eur J Med Chem 2012;58:50–63.
[50] Connelly NG, Geiger WE. Chemical redox agents for organometallic chemistry. Chem Rev 1996;96(2):877–910.
[51] Adams GE, Dewey DL. Hydrated electrons and radiobiological sensitisation. Biochem Biophys Res Commun 1963;12:473–7.
[52] Adams GE, Cooke MS. Electron-affinic sensitization. I. A structural basis for chemical radiosensitizers in bacteria. Int J Radiat Biol Relat Stud Phys Chem Med 1969;15(5):457–71.
[53] Simic M, Powers EL. Letter: correlation of the efficiencies of some radiation sensitizers and their redox potentials. Int J Radiat Biol Relat Stud Phys Chem Med 1974;26(1):87–90.
[54] Adams GE, Flockhart IR, Smithen CE, Stratford IJ, Wardman P, Watts ME. Electron-affinic sensitization. VII. A correlation between structures, one-electron reduction potentials, and efficiencies of nitroimidazoles as hypoxic cell radiosensitizers. Radiat Res 1976;67(1):9–20.
[55] Wardman P. Reduction potentials of one-electron couples involving free radicals in aqueous solution. J Phys Chem Ref Data 1989;18(4):1637–755.
[56] Breccia A, Berrilli G, Roffia S. Chemical radiosensitization of hypoxia cells and redox potentials: correlation of voltammetric results with pulse radiolysis data of nitro-compounds and radiosensitizers. Int J Radiat Biol 1979;36(1):85–9.
[57] Squella JA, Campero A, Maraver J, Carbajo J. Electrochemical reduction of 2-nitroimidazole in aprotic medium: influence of its dissociation equilibrium on the reduction mechanism. http://www.captura.uchile.cl/bitstream/handle/2250/5072/180-2006.pdf?sequence=1.
[58] Alberto R, Schibli R, Egli A, Schubiger AP. Novel organometallic aqua complex of technetium for the labeling of biomolecules: synthesis of $[^{99m}Tc(OH_2)_3(CO)_3]^+$ from $[^{99m}TcO_4]^-$ in aqueous solution and its reaction with a bifunctional ligand. J Am Chem Soc 1998;120(31):7987–8.
[59] Schibli R, La Bella R, Alberto R, Garcia-Garayoa E, Ortner K, Abram U, et al. Influence of the denticity of ligand systems on the in vitro and invivo behavior of (99 m)Tc(I)-tricarbonyl complexes: a hint for the future functionalization of biomolecules. Bioconjug Chem 2000;11(3):345–51.
[60] Banerjee SR, Babich JW, Zubieta J. Bifunctional chelates with aliphatic amine donors for labeling of biomolecules with the $\{Tc(CO)_3\}^+$ and $\{Re(CO)_3\}^+$ cores. The crystal and molecular structure of $[Re(CO)_3\text{-}\{(H_2NCH_2CH_2)_2\ N(CH_2)_4CO_2Me\}]$ Br. Inorg Chem Commun 2004;7:481–4.
[61] Troutner DE, Volkert WA, Hoffman TJ, Holmes RA. A neutral lipophilic complex of ^{99m}Tc with a multidentate amine oxime. Int J Appl Radiat Isot 1984;35(6):467–70.
[62] Lipowska M, He H, Xu X, Taylor AT, Marzilli PA, Marzilli LG. Coordination modes of multidentate ligands in fac-[Re(CO)(3)(polyaminocarboxylate)] analogues of (99 m)Tc radiopharmaceuticals. Dependence on aqueous solution reaction conditions. Inorg Chem 2010;49(7):3141–51.
[63] Adams MF, Dorie Mary Jo, Brown JM. Oxygen tension measurements of tumors growing in mice. Int J Radiat Oncol Biol Phys 1999;45(1):171–80.
[64] Pauletti GM, Okumu FW, Borchardt RT. Effect of size and charge on the passive diffusion of peptides across Caco-2 cell monolayers via the paracellular pathway. Pharm Res 1997;14(2):164–8.
[65] Craig WA, Welling PG. Protein binding of antimicrobials: clinical pharmacokinetics and therapeutic implications. Clin Pharmacokinet 1977;2(4):252–68.
[66] Jusko WJ, Gretch M. Plasma and tissue protein binding of drugs in pharmacokinetics. Drug Metab Rev 1976;5(1):43–140.
[67] Ballinger JR, Kee JW, Rauth AM. In vitro and in vivo evaluation of a technetium-99 m-labeled 2-nitroimidazole (BMS181321) as a marker of tumor hypoxia. J Nucl Med 1996;37(6):1023–31.
[68] Melo T, Duncan J, Ballinger JR, Rauth AM. BRU59-21, a second-generation ^{99m}Tc-labeled 2-nitroimidazole for imaging hypoxia in tumors. J Nucl Med 2000;41(1):169–76.
[69] Kedderis GL, Miwa GT. The metabolic activation of nitroheterocyclic therapeutic agents. Drug Metab Rev 1988;19(1):33–62.
[70] Sasai K, Iwai H, Yoshizawa T, Nishimoto S, Shibamoto Y, Kitakabu Y, et al. Pharmacokinetics of fluorinated 2-nitroimidazole hypoxic cell radiosensitizers in murine peripheral nervous tissue. Int J Radiat Biol 1992;62(2):221–7.